**Universidade de Aveiro** Departamento de Biologia
**2010**

**MÓNICA ALEXANDRA DOS SANTOS FERREIRA**

# I-2L, UM POSSÍVEL INIBIDOR DA PP1 EM ESPERMATOZÓIDES HUMANOS

# I-2L, A NOVEL PUTATIVE PP1 INHIBITOR IN HUMAN SPERM

**Universidade de Aveiro** Departamento de Biologia
**2010**

**MÓNICA ALEXANDRA DOS SANTOS FERREIRA**

# I-2L, UM POSSÍVEL INIBIDOR DA PP1 EM ESPERMATOZÓIDES HUMANOS

# I-2L, A NOVEL PUTATIVE PP1 INHIBITOR IN HUMAN SPERM

Dissertação apresentada à Universidade de Aveiro para cumprimento dos requisitos necessários à obtenção do grau de Mestre em Biologia Molecular e Celular, realizada sob a orientação científica da Professora Doutora Margarida Sâncio da Cruz Fardilha, Professora Auxiliar Convidada da Secção Autónoma de Ciências da Saúde da Universidade de Aveiro.

**o júri**

| | |
|---|---|
| presidente | Professora Doutora Maria de Lourdes Gomes Pereira<br>Professora Associada com Agregação da Universidade de Aveiro |
| orientador | Professora Doutora Margarida Sâncio da Cruz Fardilha<br>Professora Auxiliar Convidada da Universidade de Aveiro |
| arguente | Professor Doutor Filipe Almeida Monteiro<br>Professor Auxiliar Convidado da Universidade do Porto |

**agradecimentos**

Ao meu orientador, Professor Edgar da Cruz e Silva, a quem dedico este trabalho.

À minha orientadora, Professora Margarida Fardilha, pela disponibilidade, motivação e apoio oferecido durante o desenvolvimento desta dissertação.

A todos os colegas do Centro de Biologia Celular, em particular do Laboratório de Transdução de Sinais.

À minha família, em especial aos meus pais, irmã, cunhado e ao Diogo, pelo afecto partilhado ao longo de todas as etapas da minha vida.

A todos os que incentivam e alimentam a minha curiosidade.

**palavras-chave**

Fosforilação de proteínas, proteína fosfatase-1, inibidor-2, inibidor-2L, espermatozóides, (in)fertilidade masculina.

**resumo**

A proteína fosfatase-1 (PP1) é uma proteína fosfatase ubíqua e específica para a desfosforilação de resíduos de serina e treonina, que participa na regulação de diversos processos celulares. Em mamíferos, a actividade da PP1 está relacionada com a motilidade dos espermatozóides durante o percurso no tracto epididimal. Esta holoenzima é composta por uma subunidade catalítica, denominada PP1c, e por proteínas que interagem com a PP1 (PIPs) e a dirigem para a proximidade de substratos, determinando a sua actividade. A PP1 é codificada por três genes distintos: *PP1α*, *PP1β* e *PP1γ*. As isoformas PP1γ1 e PP1γ2 são originadas por splicing alternativo do gene *PP1γ*. PP1γ1 é uma isoforma ubíqua e a PP1γ2 é expressa maioritariamente no testículo e espermatozóides. O inhibidor-2 (I-2) de mamífero é uma PIP ancestral que se liga à PP1c, resultando na inibição da actividade da PP1. A reactivação deste complexo é desencadeada pela desfosforilação do I-2 no resíduo de Thr73 pela GSK-3.

Atendendo às diversas funções que têm sido atribuídas à PP1, com base nas suas subunidades reguladoras, é crucial identificar novas PIPs. Assim, com o objectivo de identificar novas PIPs em testículo humano, procedeu-se ao rastreio de uma biblioteca de cDNA de testículo humano pelo método de dois híbrido de levedura, usando a PP1γ1 e PP1γ2 como isco. Foi assim obtido um clone muito semelhante ao I-2, denominado I-2L. Após um estudo comparativo por análise bioinformática, a principal diferença detectada foi a substituição de um resíduo de Thr73 por um de Pro73, no I-2L, conduzindo à ausência do local de fosforilação pela GSK-3, o que resulta num novo mecanismo de regulação para o complexo PP1γ2-I-2L. A presença de I-2/I-2L em espermatozóides humanos foi confirmada pelos métodos de Western blot e imunocitoquímica. As proteínas I-2/I-2L e a PP1γ2 co-localizam na peça intermédia e principal do flagelo dos espermatozóides, em concordância com o papel do complexo PP1γ2-(I-2/I-2L) na motilidade dos espermatozóides. A semelhança entre o I-2 e I-2L, em termos da sequência de aminoácidos (95%), origina um novo desafio na diferenciação destas duas proteínas. Consequentemente, foi analisado o *fingerprint* proteolítico do I-2 e I-2L para posterior análise por espectrometria de massa, sendo esta uma abordagem eficaz para provar a existência do I-2L *in vivo*. Estudos estão presentemente a decorrer no sentido de validar, por espectrometria de massa, a sequência de aminoácidos do I-2L imunoprecipitado de espermatozóides humanos.

**keywords**

Protein phosphorylation, protein phosphatase-1, Inhibitor-2, Inhibitor-2L, spermatozoa, male (in)fertility.

**abstract**

Protein phosphatase-1 (PP1) is a ubiquitously expressed serine/threonine protein phosphatase that controls several cellular processes. In mammalian sperm, changes in PP1 activity correlates with sperm motility development during the transit through the epididymis. The PP1 holoenzyme structure is composed of a conserved subunit termed PP1c and PP1-interacting proteins (PIPs) which direct the holoenzyme to the proximity of its substrates, determining their activity. The catalytic subunit of PP1 is encoded by three different genes termed *PP1*α, *PP1β* and *PP1γ*. PP1γ1 and PP1γ2 are alternatively spliced isoforms of the *PP1γ* gene. PP1γ1 is ubiquitously expressed whereas PP1γ2 is mainly expressed is testis and sperm. Mammalian inhibitor-2 (I-2) is an ancient PIP that binds to PP1c, resulting in the inhibition of PP1 activity. The reactivation of this complex is triggered by phosphorylation of I-2 at Thr73 residue by GSK-3.

Given all the roles that have been proposed to PP1 based on its binding subunits it seemed very important to identify novel PIPs. Thus, in order to search for novel PP1 regulator in human testis yeast two-hybrid screens were performed using PP1γ1 and PP1γ2 as baits to screen a human testis cDNA library. A clone was obtained very similar to I-2, termed I-2 Like (I-2L). After bioinformatics analysis comparison, the main difference detected was Thr73/Pro73 substitution which abolishes the GSK-3 phosphorylation site. This introduces a new regulatory mechanism for the PP1γ2-I-2L complex. The presence of I-2/I-2L in human sperm was confirmed by immunoblot and immunocytochemistry analysis. I-2/I-2L and PP1γ2 co-localize endogenously in the middle- and principal- piece of spermatozoa flagellum consistent with the role of PP1γ2-(I-2/I-2L) complex in sperm motility. The similarities between I-2/I-2L in terms of amino acid sequences (95%) introduced a challenge to differentiate I-2 and I-2L proteins. Hence, the proteolytic *fingerprint* of I-2 and I-2L was analyzed for further mass spectrometry (MS) analysis, and concluded that this was a fine approach to prove the existence of I-2L *in vivo*. Studies are now in progress in order to validate, via MS analysis, the amino acid sequence of I-2L immunoprecipitated from human sperm.

Abbreviations ..... 8
1. Introduction ..... 11
1.1. Protein phosphorylation ..... 12
1.2. Protein phosphatases ..... 13
1.2.1. Recognition of substrates by protein phosphatases ..... 14
1.2.2. Protein Phosphatase 1 (PP1) ..... 14
1.2.3. Protein Phosphatase 1 Inhibitors ..... 19
1.2.4. Yeast two-hybrid (YTH) system ..... 25
1.3. Aims of this thesis ..... 27
2. Bioinformatics analysis of I-2L ..... 29
2.1. Identification of Inhibitor-2 Like and comparison with Inhibitor-2 ..... 30
2.2. Peptide fragments predicted from tryptic digestion ..... 33
3. Detection and identification of I-2L as a novel putative protein ..... 35
3.1. Expression of endogenous I-2/I-2L in human and rat tissues ..... 36
3.1.1. Introduction ..... 36
3.1.2. Materials and Methods ..... 37
3.1.3. Results ..... 43
3.1.4. Discussion ..... 45
3.2. Co-localization of I-2/I-2L with PP1γ2 isoform in human spermatozoa ..... 47
3.2.1. Introduction ..... 47
3.2.2. Material and Methods ..... 48
3.2.3. Results ..... 50
3.2.4. Discussion ..... 52
3.3. Immunoprecipitation of I-2/I-2L and mass spectrometry analysis ..... 55
3.3.1. Introduction ..... 55
3.3.2. Material and Methods ..... 56
3.3.3. Results ..... 59
3.3.4. Discussion ..... 63
4. Discussion and Perspectives ..... 65
5. References ..... 71
Appendix ..... 81

## Abbreviations

| | |
|---|---|
| aa | Amino acid |
| AC | Adenylyl cyclase |
| Ade | Adenine |
| ADP | Adenosine diphosphate |
| APS | Ammonium persulfate |
| ATP | Adenosine triphosphate |
| AKAP4 | A-kinase-anchoring protein 4 |
| Arg | Arginine |
| BCA | Bicinchoninic acid |
| BLAST | Basic Local Alignment Search Tool |
| BM | Binding motif |
| BSA | Bovine serum albumin |
| cAMP | Cyclic AMP (Adenosine 3´, 5´-monophosphate) |
| cDNA | Complementary deoxyribonucleic acid |
| Cdk | Cyclin-dependent kinase |
| Cdk 5 | Cyclin-dependent kinase 5 |
| CKII | Casein kinase II |
| Da | Dalton |
| DARPP-32 | Dopamine and cAMP-regulated phosphoprotein 32 kDa |
| DNA | Deoxyribonucleic acid |
| ECL | Enhanced chemiluminescence |
| ELM | Eukaryote Linear Motif resource |
| FITC | Fluorescein isothiocyanate |
| GAL4 | Gal4 transcription factor |
| GAL4-AD | Gal4 activation domain |
| GAL4-BD | Gal4 DNA binding domain |
| GSK-3 | Glycogen synthetase kinase 3 |
| His | Histidine |
| Hr | Hour |
| I-1 | Inhibitor-1 |
| I-2 | Inhibitor-2 |

| | |
|---|---|
| I-2L | Inhibitor-2 Like |
| I-3 | Inhibitor-3 |
| I-4 | Inhibitor-4 |
| IP | Immunoprecipitation |
| IUPs | Intrinsically unstructured proteins |
| K | Lysine |
| LB | Loading buffer |
| Leu | Leucine |
| LGB | Lower gel buffer |
| Lys | Lysine |
| min | Minute |
| mRNA | Messenger ribonucleic acid |
| MAPK | Mitogen-activated protein kinase |
| MYPT | Myosin phosphatase targeting subunit |
| MS | Mass spectrometry |
| NCB | Non-capacitating buffer |
| Nek2 | NimA-related protein kinase |
| OD | Optical density |
| PBS | Phosphate buffered saline |
| PI3 | Phosphatidyl inositol kinase-3 |
| PIPs | PP1-interacting proteins |
| PKA | Protein kinase A |
| PKB | Protein kinase B |
| PKC | $Ca^{2+}$/phospholipid-activated protein kinase |
| PP1 | Protein phosphatase 1 |
| PP2A | Protein phosphatase 2A |
| PP1c | Protein phosphatase 1 catalytic subunit |
| PPM | Metal ion dependent protein phosphatase |
| PPP | Phosphoprotein phosphatase |
| Pro | Proline |
| PTP | Tyrosine protein phosphatase |
| R | Arginine |
| RNA | Ribonucleic acid |
| RT | Room temperature |
| SDS | Sodium dodecyl sulphate |

| | |
|---|---|
| SDS-PAGE | Sodium dodecyl sulphate – polyacrylamide gel electrophoresis |
| Sec | Seconds |
| Ser | Serine |
| TBS | Tris-buffered saline solution |
| TBST | TBS supplemented with Tween detergent |
| TEMED | N, N, N´, N' - Tetramethylethylenediamine |
| Thr | Threonine |
| Trp | Tryptophan |
| Tyr | Tyrosine |
| UAS | Upstream activating sequence |
| UGB | Upper gel buffer |
| WR | Working reagent |
| X-α-gal | 5-bromo-4-chloro-3-indolyl-alpha-D-galactopyranoside |
| YTH | Yeast two-hybrid |

# 1. Introduction

## 1.1. Protein phosphorylation

The reversible phosphorylation of proteins is a major intracellular control mechanism involved in a wide range of eukaryotic cellular responses. The control of biological events requires strict regulation using complex protein phosphorylation and dephosphorylation strategies. Phosphorylation is mediated by the coordinated action of protein kinases and phosphatases (Hurley *et al*., 2007). The reversible protein phosphorylation involves either the addition of a phosphate group via the transference of the terminal phosphate from ATP to an amino acid residue by protein kinases or its removal by protein phosphatases (Figure 1).

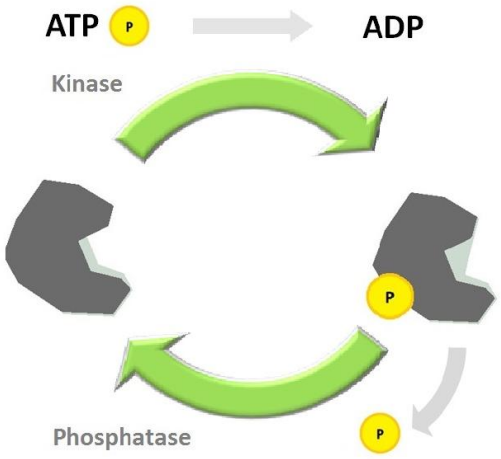


**Figure 1:** Schematic representation of reversible protein phosphorylation. Protein kinase moves a phosphate group from ATP to a target protein (protein phosphorylation) while a protein phosphatase catalyzes the removal of the phosphate group from the target protein (protein dephosphorylation).

The importance of phosphorylation networks in eukaryotes is underscored by the estimated one-third of cellular proteins that are phosphorylated, with the vast majority of the modifications occurring on tyrosine, serine and threonine residues (Virshup and Shenolikar, 2009). The protein phosphorylation (or dephosphorylation) on these amino acid residues causes conformational changes in proteins, modifying their biological properties (Bollen, 2001; Ceulemans and Bollen, 2004).

Eukaryotic cells express various protein kinases and phosphatases, which have specific substrates, cellular localizations and regulation mechanisms. Whereas the number of tyrosine phosphatases is approximately the same of tyrosine kinases, the number of serine/threonine kinases is higher to that of serine/threonine phosphatases (Bollen, 2001; Ceulemans and Bollen, 2004). It is known that more than 400 human genes encode protein serine/threonine kinases but there are only about 40 genes that encode protein serine/threonine phosphatases. It seems that the protein kinases had mainly diversified by gene duplication and subsequent specification, whereas proteins serine/threonine phosphatases have diversified much more by increasing the variety of their regulatory subunits (Hendrickx *et al*., 2009).

## 1.2. Protein phosphatases

Protein phosphatases belong to three unrelated gene families: the PPM family (metal ion dependent protein phosphatases), the PTP family (tyrosine protein phosphatases) and the PPP family (phosphoprotein phosphatases). The PPP family members comprise the serine/threonine phosphatases PP1, PP2A, PP2B, PP4, PP5, PP6 and PP7 (Honkamen and Golden, 2002; Virshup and Shenolikar, 2009).

A key defining feature of most PPP family members is that they are multimeric enzymes. No more than 13 human genes encode PPP catalytic subunits, which are associated with numerous PPP regulatory subunits that do not share extensive sequence conservation. Instead, they are identified by their physical association and function that provide the critical determinants for subcellular localization, substrate specificity, and fine-tuning of phosphatase activity. Hence, these regulatory proteins confer remarkable complexity to protein phosphatases. Added to these regulatory subunits, an increasing number of PPP inhibitory proteins also control cell dephosphorylation capacity (Virshup and Shenolikar, 2009).

### 1.2.1. Recognition of substrates by protein phosphatases

Serine/threonine-specific protein phosphatases (PPs) can be classified into different types on the bases of their substrate specificity and responses to a defined set of inhibitors and activators (Ingebritsen and Cohen, 1983). These criteria define four types of catalytic protein phosphatases: PP1, PP2A, PP2B and PP2C. PP1 can be distinguished from the other types by its sensitivity to two heat-stable inhibitors, I-1 and I-2 (Vijayaraghavan *et al*., 1996), and type 2 PPs can be sub-classified into PP2A, PP2B, and PP2C based on cation requirements. PP1 and PP2A do not require divalent cations for activity whereas PP2B and PP2C require $Ca^{2+}$/calmodulin and $Mg^{2+}$, respectively, for activity (Smith *et al*., 1996). Furthermore, techniques such as yeast two-hybrid (YTH) assays and co-immunoprecipitation (Co-IP) suggested that a physical association with phosphatases may be a hallmark of all substrates, and that the binding of phosphatases to substrates narrows their substrate specificity, limiting them to dephosphorylate a subset of the phosphorylated amino acids in the target peptide sequence that interacts with both the regulatory and catalytic subunits (Virshup and Shenolikar, 2009).

### 1.2.2. Protein Phosphatase 1 (PP1)

Protein phosphatase-1 (PP1) is a ubiquitous and conserved enzyme that is estimated to catalyze a third of all protein dephosphorylations in eukaryotic cells (Hendrickx *et al*., 2009). This major serine/threonine protein phosphatase controls several cellular processes such as glycogen metabolism, muscle contraction, cell cycle, gene expression, and neuronal activity (reviewed in Virshup and Shenolikar, 2009). In mammalian sperm, a change in PP1 activity correlates with sperm motility development during the transit through the epididymis, consistent with a major role for PP1 in the control of this process (Vijayaraghavan *et al*., 1996). PP1 interacts with dozens of regulatory proteins, and its function is associated with regulatory components that direct the enzyme to various sub-cellular compartments in the proximity of substrates and modulate the phosphatase activity (Fardilha *et al*., 2010).

### 1.2.2.1. PP1 catalytic and regulatory subunits

PP1 holoenzymes are composed of a highly conserved catalytic subunit termed Protein Phosphatase 1 catalytic subunit (PP1c) and one or two regulatory (R) subunits (Bollen, 2001). Although the activity of PP1c can be regulated by cell cycle dependent dephosphorylation of serine/threonine residues in its C-terminus, the regulation of PP1 holoenzymes by extracellular signals is mainly mediate by the R subunits (Bollen, 2001). The catalytic subunit of PP1 can be encoded by three different genes, termed *PP1α, PP1δ/β,* and *PP1γ* (Hurley *et al*., 2007; Smith *et al*., 1996). Figure 2 shows an amino acid sequence alignment of the different PP1c isoforms. Two isoforms of PP1γ, PP1γ1 and PP1γ2, are alternatively spliced isoforms generated from a single gene. This two variants are identical in all respects, except that PP1γ2 has a unique 21 amino acid carboxyl terminus extension (da Cruz e Silva *et al.,* 1995; Zhang *et al*., 1993). PP1γ1 is ubiquitously expressed, whereas PP1γ2 is expressed mainly in the testis and spermatozoa (Huang and Vijayaraghavan, 2004; Smith *et al*., 1996; Vijayaraghavan *et al*., 1996).

```
PP1gamma1       MADLDKLNIDSIIQRLLEVRGSKPGKNVQLQENEIRGLCLKSREIFLSQPILLELEAPLK 60
PP1gamma2       MADLDKLNIDSIIQRLLEVRGSKPGKNVQLQENEIRGLCLKSREIFLSQPILLELEAPLK 60
PP1alpha        MSDSEKLNLDSIIGRLLEVQGSRPGKNVQLTENEIRGLCLKSREIFLSQPILLELEAPLK 60
PP1beta         MADG-ELNVDSLITRLLEVRGCRPGKIVQMTEAEVRGLCIKSREIFLSQPILLELEAPLK 59
                *:*  :**:**:* *****:*.:*** **: * *:****:********************

PP1gamma1       ICGDIHGQYYDLLRLFEYGGFPPESNYLFLGDYVDRGKQSLETICLLLAYKIKYPENFFL 120
PP1gamma2       ICGDIHGQYYDLLRLFEYGGFPPESNYLFLGDYVDRGKQSLETICLLLAYKIKYPENFFL 120
PP1alpha        ICGDIHGQYYDLLRLFEYGGFPPESNYLFLGDYVDRGKQSLETICLLLAYKIKYPENFFL 120
PP1beta         ICGDIHGQYTDLLRLFEYGGFPPEANYLFLGDYVDRGKQSLETICLLLAYKIKYPENFFL 119
                ********* **************:************************************

PP1gamma1       LRGNHECASINRIYGFYDECKRRYNIKLWKTFTDCFNCLPIAAIVDEKIFCCHGGLSPDL 180
PP1gamma2       LRGNHECASINRIYGFYDECKRRYNIKLWKTFTDCFNCLPIAAIVDEKIFCCHGGLSPDL 180
PP1alpha        LRGNHECASINRIYGFYDECKRRYNIKLWKTFTDCFNCLPIAAIVDEKIFCCHGGLSPDL 180
PP1beta         LRGNHECASINRIYGFYDECKRRFNIKLWKTFTDCFNCLPIAAIVDEKIFCCHGGLSPDL 179
                ***********************:************************************

PP1gamma1       QSMEQIRRIMRPTDVPDQGLLCDLLWSDPDKDVLGWGENDRGVSFTFGAEVVAKFLHKHD 240
PP1gamma2       QSMEQIRRIMRPTDVPDQGLLCDLLWSDPDKDVLGWGENDRGVSFTFGAEVVAKFLHKHD 240
PP1alpha        QSMEQIRRIMRPTDVPDQGLLCDLLWSDPDKDVQGWGENDRGVSFTFGAEVVAKFLHKHD 240
PP1beta         QSMEQIRRIMRPTDVPDTGLLCDLLWSDPDKDVQGWGENDRGVSFTFGADVVSKFLNRHD 239
                ***************** *************** ****************:**:***::**

PP1gamma1       LDLICRAHQVVEDGYEFFAKRQLVTLFSAPNYCGEFDNAGAMMSVDETLMCSFQILKPAE 300
PP1gamma2       LDLICRAHQVVEDGYEFFAKRQLVTLFSAPNYCGEFDNAGAMMSVDETLMCSFQILKPAE 300
PP1alpha        LDLICRAHQVVEDGYEFFAKRQLVTLFSAPNYCGEFDNAGAMMSVDETLMCSFQILKPAD 300
PP1beta         LDLICRAHQVVEDGYEFFAKRQLVTLFSAPNYCGEFDNAGGMMSVDETLMCSFQILKPSE 299
                ************************************.*****************::

PP1gamma1       KKK---------PNATRPVTPPRG------MITKQAKK-------- 323
PP1gamma2       KKK---------PNATRPVTPPRVGSGLNPSIQKASNYRNNTVLYE 337
PP1alpha        KNKGKYGQFSGLNPGGRPITPPRN-------SAKAKK--------- 330
PP1beta         KKAKYQYG---GLNSGRPVTPPRT--------ANPPKKR------- 327
```

**Figure 2:** Analysis of homology of PP1 isoforms using a CLUSTALW multiple sequence alignment.

Mammalian PP1 isoforms do not exist freely in the cell but tightly associate with different interactors (Figure 3) that determine when and where the phosphatase acts (Hurley *et al*., 2007). Based on the effect on PP1c, the best-characterized R subunits can be generally divided into three groups; a group represented by activity-modulating proteins, including the inhibitor-1, inhibitor-2 and inhibitor-4 that, depending on their phosphorylated state, block the activity of PP1c (Figure 3 and 4), a group of R subunits contains the targeting proteins which binds both PP1c and one of the substrates, for example, MYPT1 binds PP1c as well as specific substrates such as myosin, and finally, a group of proteins that directly and tightly associates with PP1c, defining a subset of its substrates that can function as activity modulators (Bollen, 2001; Hendrickx *et al*., 2009).

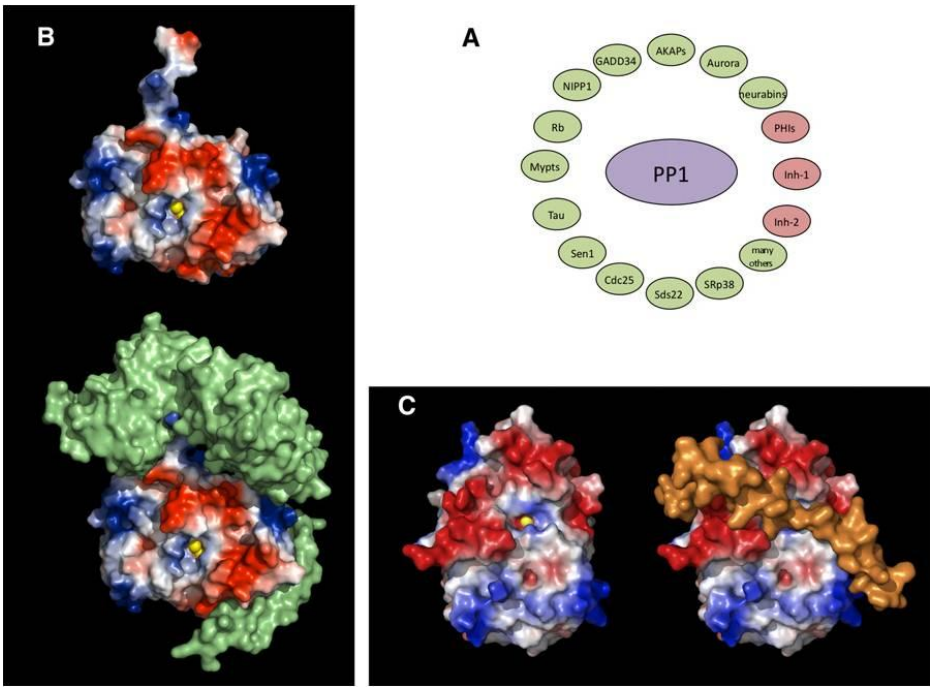


**Figure 3:** Regulation of protein phosphatase 1. **A**|Protein phosphatase 1 is controlled by regulatory interactions (green) and inhibitors (orange). **B**|Regulatory interactions control the entrance of the substrate in to the catalytic site. PP1β is represented without and with MYPT1 subunit. The catalytic metals in the active site are shown in yellow, PP1 is represented with electrostatic potential, and MYPT1 in green. The interaction of MYPT1 with PP1 stabilizes its flexible C-terminus that extends from the PP1 catalytic subunit. **C**|A PP1 inhibitor physically blocks the active site. PP1γ1 without or with inhibitor-2 (I-2) (orange) is depicted with the catalytic subunits (adapted from Virshup and Shenolikar, 2009).

It has been demonstrated that the binding of R subunits to PP1c is mediated by multiple, degenerated, short sequence motifs and that the R subunits can share interaction sites in a combinatorial control of PP1c (Figure 4) (Bollen, 2001).

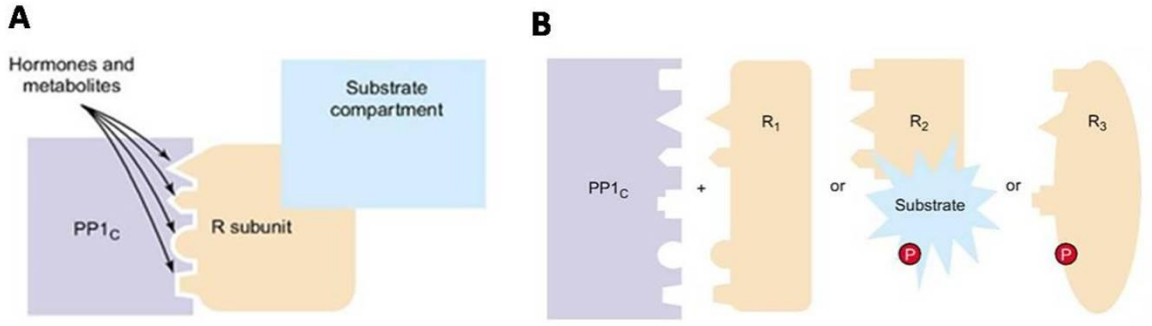


**Figure 4: A**| Schematic structure of protein phosphatase 1 (PP1) holoenzymes. PP1c has multiple points of interaction with a regulatory subunit (R), which direct the holoenzyme in proximity to its substrates, determining its activity. Hormones and metabolites modulate the substrate actions, controlling PP1 holoenzyme. **B**| Combinatorial-control model of PP1c is represented with different binding sites for R subunits. The R subunits are activity modulators (R1), targeting proteins (R2) and substrates (R3). These R subunits have multiple contacts with PP1c binding sites, contributing for the specificity with the binding products on PP1c (adapted from Bollen, 2001).

The regulatory proteins are structurally unrelated, but most of them share a short, degenerate RVXF-type docking motif that binds to a hydrophobic surface groove located on a surface behind the PP1c active site (Hendrickx *et al*., 2009; Virshup and Shenolikar, 2009), which has a consensus (R/K) $X_{A\ (0\text{-}1)}$ (V/I)$X_B$ (F/W) sequence, where $X_A$ is any amino acid, present or absent, and $X_B$ is any amino acid, except proline. The binding of the RVXF sequence to PP1c does not cause important conformational changes of the catalytic subunit but increases the local concentration of the interactor (Hendrickx *et al*., 2009).

Studies on MYPT1 and I-2 (Figure 5) indicated that the RVXF motif can function as an anchor for PP1c and enables these R subunits to make additional contacts with the PP1 in a cooperative manner.

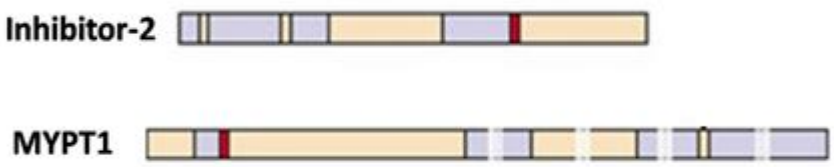


**Figure 5:** Representation of Inhibitor-2 and MYPT1 sites that mediate the interaction of the regulatory subunits (blue bars) with the catalytic subunits of PP1c. The RVXF motifs are shown in red and extra phosphatase-interaction sites are represented in beige (adapted from Bollen, 2001).

Moreover, the RVXF-binding pocket is surrounded by acidic residues that might provide additional binding sites for the basic residues often found N-terminally to the RVXF motif. Other surface areas of PP1c that interact with R subunits are the catalytic site and the β12-β13 loop. In addition, the site that lies adjacent to the RVXF binding groove (Figure 6) has been identified as a binding pocket for the N-terminal K[GS]ILK motif of I-2 (Bollen, 2001; Wakula, 2003).

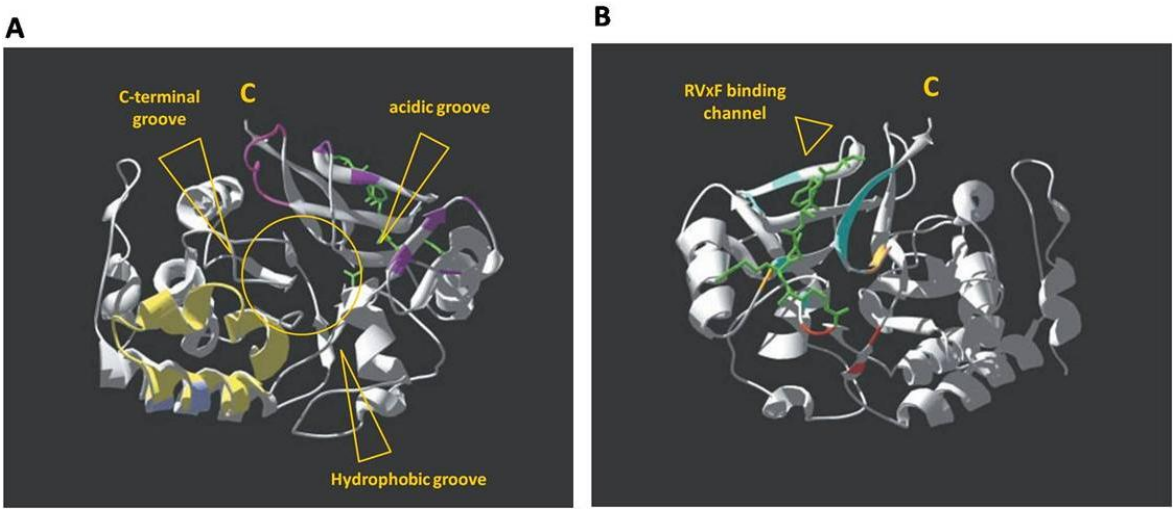


**Figure 6:** Structure of PP1γ (ribbons) bound to an RVXF-containing peptide. **A**| Frontal sight of PP1 with three grooves originated from the catalytic site. The β12/β13 loop is drawn at magenta and the α4/α5 /α6 triangle in yellow. The acidic residues from the acidic groove are shown in purple. **B**| Dorsal view of PP1 with its catalytic site. The RVXF-containing peptide is represented in green. The cooperative RVXF-binding channel is lined by residues of the β-strand, β14 and the neighboring residues (blue). The protein surface near the channel, which bind the basic residues prior to the V-position of the RVXF-motif, is negative charged due to the acidic residues (red and orange). Some of these residues (red) are also related with K[GS]ILK-motif of I-2 (adapted from Ceulemans and Bollen, 2004).

Recent analysis of RVXF-based PP1 interactome provided new insights into the conserved features of the RVXF motif and led to the discovery of additional common PP1 binding elements, described as the SILK-motif:[GS]-IL-[RK] and MyPhoNE-motif (reviewed in Hendrickx *et al*., 2009). One of the PP1docking motifs of I-2 matches to that consensus sequence [GS]-IL-[RK] indicating that the SILK-motif is essential for the potent PP1 inhibition by I-2 (Hurley *et al*., 2007). Hendrickx *et al*. (2009) found that the SILK-motif also occurs in six other PP1 interactors and is always N-terminal to the RVXF-motif and that the importance of this motif for the anchoring of PP1 is interactor dependent.

### 1.2.3. Protein Phosphatase 1 Inhibitors

#### 1.2.3.1. Heat-stable Protein Phosphates 1 Inhibitors

PP1 binds to a number of small cytosolic inhibitory proteins (Li *et al*., 2007), including inhibitor-1 (I-1) and its isoform dopamine and cAMP- regulated phosphoprotein 32 kDa (DARPP-32), inhibitor-2 (I-2), the mammalian smooth muscle specific PP1 inhibitor CPI17, human HCG V gene product (inhibitor-3), the testis-specific PP1 inhibitor from *Drosophila melanogaster* that has 41% sequence similarity to mammalian I-2 (inhibitor-t), and Glc8p that is a homologue of I-2 from *Saccharomyces cerevisiae* (Helps and Cohen, 1999). Effectively, the family of I-2 proteins exhibits considerable sequence variation, with I-2 from non-vertebrate species having only 30% identity with I-2 from vertebrates (Li *et al*., 2007). Despite these divergences in sequence, all these I-2 proteins have the same size (187-229 residues) and are heat stable, possibly due to the presence of charged and hydrophilic amino acid residues.

I-2 family members have multiple phosphorylation sites for different kinases, such as Casein kinase II (CKII) (Li *et al*., 2007), the neuronal Cdc2-like protein kinase (NCLK), a heterodimer of Cdk5 and the regulatory p25 (Agarwal-Mawal and Paudel, 2001), the extracellular signal-regulated kinases (ERKs), the cyclin-dependent kinases (CDKs) (Hurley *et al*., 2007), and Glycogen synthase kinase-3 (GSK-3), which is highly specific for *Drosophila melanogaster* I-2 and *Homo sapiens* I-2 (Li *et al*., 2007). I-2 is also related to the regulation of other kinases that are complexed with PP1 during the cell cycle, activating the NimA-related kinase, Nek-2, to induce centrosome separation (Eto *et al*.,

2002). Also, I-2 stimulates the Aurora-A kinase that is necessary for the centrosome maturation, assembly of the bipolar spindle, and proper chromosome segregation during cell division (Satinover *et al*., 2004).

PP1 is sensitive to endogenous I-1 and I-2 whereas PP2 is insensitive. Comparatively, the inactivation of PP1 by I-1 is dependent on I-1 phosphorylation of a single threonine residue by cAMP-dependent protein kinase A (PKA), and by $Ca^{2+}$/calmodulin-dependent dephosphorylation by PP2B, while I-2 does not necessarily require phosphorylation for PP1 inhibition (Smith *et al*., 1999; Vijayaraghavan *et al*., 1996). The inhibition of PP1 by I-2 occurs through the binding to the catalytic subunit of PP1 to form an inactive cytoplasm form of the enzyme (PP1-I-2) that can be converted to active PP1 by phosphorylation of the bound I-2 by GSK-3 and other kinases (Smith *et al*., 1996; 1999; Vijayaraghavan *et al*., 1996).

#### 1.2.3.2. GSK-3 protein kinase phosphorylates I-2

GSK-3 is a ubiquitously expressed magnesium-adenosine triphosphate (Mg-ATP)-dependent enzyme, with the two isoforms GSK-3α and GSK-3β being expressed in somatic cells (King *et al*., 2006). GSK-3 activity can be regulated by tyrosine and serine/threonine phosphorylation. Tyrosine phosphorylation increases GSK-3 catalytic activity. Serine/threonine phosphorylation is mediated by phosphatidyl inositol kinase-3 (PI3-kinase) and protein kinase B (PKB) (King *et al*., 2006). The PI3-kinase, activated by cell adhesion, growth factors, and insulin, in turn activates PKB, which results in phosphorylation and inactivation of GSK-3 (Vijayaraghavan *et al*., 1996; 2000). Thus, GSK-3 has important functions in cellular signal transduction, like the activation of PP1 accomplished through phosphorylation of I-2 on a threonine residue, resulting in the reactivation of the PP1-I-2 complex (Vijayaraghavan *et al*., 2000).

### 1.2.3.3. Protein phosphatase 1 Inhibitor-2

Inhibitor-2 (I-2) is the most ancient PP1 regulatory protein, conserved from yeast to human (Li *et al*., 2007). Mammalian I-2 forms a stable and high affinity complex with PP1c termed ATP-$Mg^{2+}$-dependent phosphatase complex. I-2 promotes a slower inactivation of PP1c to create a latent complex. The reactivation of this PP1c-I-2 complex is triggered by phosphorylation of the rabbit I-2 isoform at Thr72 residue by several protein kinases (described before), including the GSK-3 kinase (Hurley *et al*., 2007).

### 1.2.3.4. Structure of PP1-Inhibitor-2 Complex

The molecular basis by which I-2 modulates PP1 function is crucial for establishing the physiological role of PP1-I-2 complex and assessing the involvement of cell dynamic control of this protein phosphatase complex. The analysis of PP1-I-2 complex structure (Figure 7) highlights common structural determinants that mediate the inactivation of PP1c by I-2 and the inhibition of other serine/threonine phosphatases (Hurley *et al*., 2007).

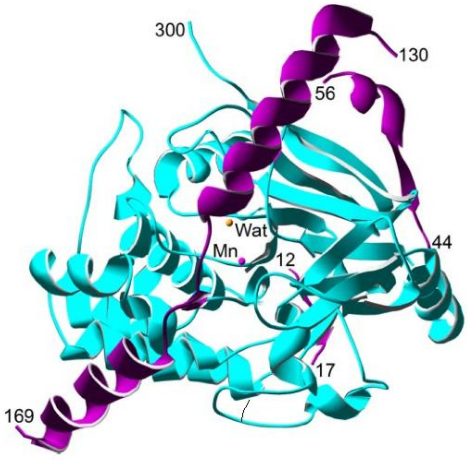


**Figure 7:** Crystal representation of the PP1cγ-I-2 complex. Ribbon structure of PP1cγ is depicted in *blue*, and that of I-2 is in *magenta*. Residue numbers indicate the start and the end positions for the observed regions of I-2, in addition to the last residue observed for PP1cγ (300). The location of the remaining catalytic manganese ion is indicated (Mn), plus the position of the water molecule (Wat) (adapted from Hurley *et al*., 2007).

Studies on cocrystallization of PP1 with I-2 (Figure 7) shows that I-2 physically occludes the catalytic site displacing two catalytic metal ions to generate an inactive or latent enzyme. This inhibition can also be regulated. The phosphorylation of I-2 by GSK-3, and other kinases, restores PP1 activity, interestingly, without releasing I-2 from PP1 (Virshup and Shenolikar, 2009). The close analysis on the PP1c-I-2 complex demonstrate that I-2, which lacked significant ordered structure, interacts with PP1c (Figure 8) to induce conformations that specifically enhances the formation of the PP1c-I-2 complex, not to modify the overall structure of PP1c, but to direct the association with the catalytic center and its ability to displace critical catalytic metals, providing the slower inactivation of PP1c (Hurley *et al*., 2007).

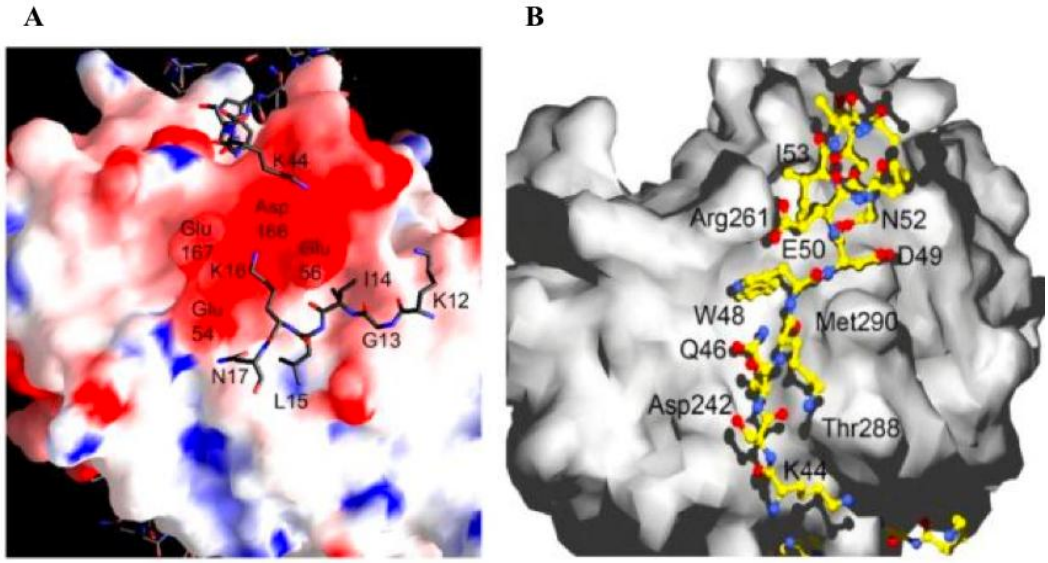


**Figure 8:** Interactions of I-2 residues 12-17 and 44-56 with PP1cγ. A | Surface representation of PP1cγ demonstrates the interaction between the I-2 residues 12-17 and the surface of PP1cγ. **B** | Region of PP1cγ to which residues 44-46 from I-2 bound. The characteristic surface PP1cγ is represented in *grey* and the structure of I-2 is represented using atom-type colouring (adapted from Hurley *et al*., 2007).

### 1.2.3.5. Inhibitor-2 in human sperm

Mammalian spermatozoa acquire their capacity for motility and fertilization during epididymal transit while concomitantly undergoes marked changes in chemical and physical properties. These changes are in shape, metabolic patterns, enzymatic activities, chemical and physical properties of the plasma membrane, ability to bind specific epididymal proteins, and in the female tract, aptitude to bind to the zona pellucida (Huang and Vijayaraghavan, 2004).

Sperm motility and fertilization involves changes in protein phosphorylation, which is a balance between the action of protein kinases and phosphatases (Vijayaraghavan *et al*., 2000). Sperm motility in immature spermatozoa can be initiated by treatments that stimulate protein kinase activity or inhibit protein phosphatase activity, suggesting that the potential for motility already exists in immature epididymal spermatozoa (Huang and Vijayaraghavan, 1996; 2004). During the passage through the epididymis, changes are observed in the intrasperm levels of cAMP, pH, and the calcium, mediators known to regulate the kinetic activity of mammalian sperm, and that presumably act through protein phosphorylation (Huang and Vijayaraghavan, 2004). Remarkably, these development changes that sperm undergo in the male epididymis occur in the absence of transcriptional or translational activity, and involve reversible phosphorylation of key proteins regulating sperm kinetic activity and metabolism (Vijayaraghavan *et al*., 1996).

Sperm protein phosphorylation is directly related to motility, and it is increased by agents that elevate sperm cAMP levels. A key enzyme regulating sperm motility development is PP1γ2, which is one isoform of PP1. High catalytic activity of sperm PP1γ2 holds the motility in check in immature caput epididymal spermatozoa. Protein phosphatase inhibitors initiate motility in caput epididymal spermatozoa and stimulate motility in caudal epididymal spermatozoa (Huang and Vijayaraghavan, 2004). Given that PP1γ2 is testis-enriched and the major isoform of PP1 in spermatozoa (Fardilha *et al*., 2004; Vijayaraghavan *et al*., 1996; 2000), it is acknowledged that PP1γ2 is essential for spermatogenesis and it is also a key enzyme in the development and regulation of sperm motility (Fardilha *et al*., 2004; Huang and Vijayaraghavan, 2004; Wu *et al*., 2007).

Sperm PP1 catalytic activity is regulated by its interaction with I-2 that resembles the one found in somatic cells (Vijayaraghavan *et al*., 2000). Of the known PP1 inhibitors, only an I-2-like activity is detected in mammalian sperm. Both human and monkey sperm contain the so named I-2-like activity as well as Mg-ATP-dependent GSK-3 activity (Smith *et al*., 1999). Once more, the inactive PP1γ2-I-2 complex is activated by phosphorylation of this I-2-like activity by GSK-3 (Vijayaraghavan *et al*., 2000). In Figure 9 is represented the role of PP1γ2-I-2 complex in sperm motility. In caput human sperm, high GSK-3 activity levels induce phosphorylation of I-2 at the Thr73 residue, which in turn, enhances the PP1γ2 activity responsible for the lack of motility. Along the epididymis, the decrease of GSK-3 activity enhances the formation of the PP1γ2-I-2 complex that promotes the initiation of sperm motility in the epididymis by the inactivation of PP1γ2.

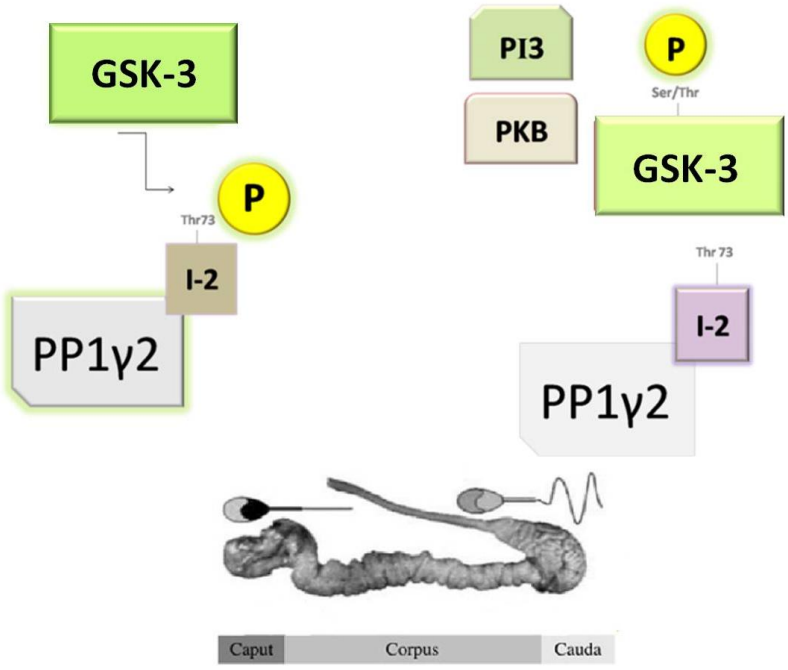


**Figure 9:** Schematic illustration of the PP1γ2-I-2 complex and its role in sperm motility. The binding of I-2 to PP1γ2 leads to the initiation of sperm motility in immature spermatozoa during epididymal transit. Serine/threonine phosphorylation decreases GSK-3 activity, enhancing the association of the PP1γ2-I-2 complex, which in turn results in the activation of sperm motility.

### 1.2.4. Yeast two-hybrid (YTH) system

Macromolecular interactions such protein-protein interactions are fundamental for all biological processes, including the regulation of signalling pathways (Lalonde *et al*., 2008). The yeast two-hybrid (YTH) method is effective for the detection of these interactions (Koegl and Uetz, 2008). The two-hybrid system is able to detect the interaction between two proteins via transcriptional activation of one or several reporter genes and is also used for searching for new partners (the prey) of a given protein (the bait) (Figure 10).

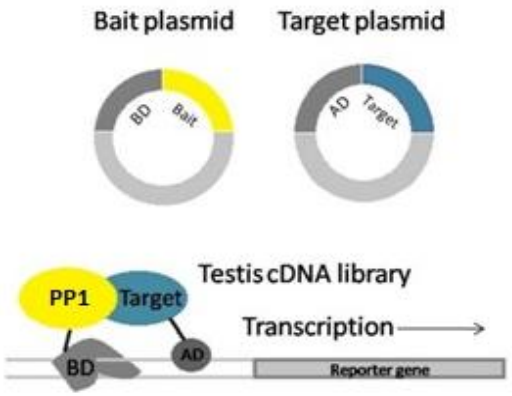


**Figure 10:** General overview of the yeast two-hybrid system. The bait (PP1) is fused to the DNA binding domain and the target protein (sequence from a testis cDNA library) is fused to the activation domain. If the bait and prey interact, the GAL4 binding domain (BD) and the GAL4 activation domain (AD) are brought together forming a functional transcriptional activator which leads to the transcriptional activation of a downstream reporter gene (adapted from Berggard *et al*., 2007).

This method is based on the properties of the yeast GAL4 protein, which has two separable domains, one responsible for DNA binding and other for transcriptional activation. YTH assay is performed by expressing the two fusion proteins in yeast. The first contain the GAL4 DNA binding domain (BD) fused in-frame to bait protein and the other contains the GAL4 activation domain (AD) fused in frame to a target protein (the prey). The prey and bait constructs are introduced, by co-transformation or mating, into yeast strains containing the appropriate "Upstream Activating Sequence" (UAS) proximal to a reporter gene. When the bait and the target protein interact, the BD and the AD are

brought together forming a functional transcriptional activator which leads to the transcriptional activation of the reporter gene. Each *GAL4* responsive gene contains a UAS target site, when GAL4 binds the UAS transcription is activated from a downstream promoter. By linking the GAL4 UAS with other metabolic genes (e.g. ADE2, HIS3, MEL1 and lacZ) and by eliminating the wild type *GAL* gene, researchers have developed yeast strains that change phenotype when GAL4 is activated. Although the GAL4 DNA-BD can bind the UAS, it cannot activate transcription by itself. Transcription is activated only when the other half of the protein, GAL4 AD, joins the DNA-BD at the UAS. When using a large scale screen, a plasmid library, expressing cDNA-encoded AD-fusion proteins, can be screened by introduction into a yeast strain. These larger scale two-hybrid approaches typically rely on interaction by yeast mating (Parrish *et al*, 2006).

The advantages of this method are the simplicity, the minor optimization requirement, and its ability to detect proteins interactions *in vivo* (Parrish *et al*., 2006). However this method may generate false positives. Even though two proteins can interact, it is not certain that they will interact in physiological conditions. Therefore, the biological relevance of the proteins identified must be confirmed using alternative methodology such as Co-IP and overlay (Koegl and Uetz, 2008).

In order to identify proteins from a human testis cDNA library capable of interacting with the alternative spliced isoforms of PP1γ, PP1γ1 or PPγ2, two separate YTH screens were performed, YTH1 and YTH2, respectively. These isoforms are identical except for the C-terminus (Figure 2). PP1γ1 and PP1γ2 were used as baits and this methodology was used to screen a testis cDNA library (Figure 10). The binding domain plasmid carries the yeast TRP1 gene and the PP1γ1, or PP1γ2, sequence (the bait) fused to the GAL4 BD. The activation domain plasmid carries the yeast LEU2 gene and a sequence from the cDNA library (the prey) fused to the GAL4 AD. The reporter genes used were *MEL*-1 which encodes α-Galactosidase and HIS3 and ADE4. The plasmids are transformed in yeast strain which requires tryptophan (trp), leucine (leu), histidine (his) and adenine (ade). If the two proteins (the bait and the prey) interact, the reporter genes will be activated and the yeast will grow on synthetic complex medium lacking the amino acids trp, leu, his and ade. The α-Galactosidase activity is detected by the formation of blue

yeast colonies on medium with the cromogenic substrate X-α-Gal (5-bromo-4-chloro-3-indolyl alpha-D-galactopyranoside).

From the testis cDNA library, using PP1γ1 as bait (YTH1), were collected and identified 120 true positive clones. One of these clones, named 48T, was identified as a novel PP1γ1 binding protein (NM_206858), termed I-2L.

### 1.3. Aims of this thesis

PP1 multiple functions rely on its binding partners, PP1 interacting proteins (PIPs) that specify its location, preferable substrates and its activity status. The identification of novel PIPs is a mean of attributing new functions to PP1 catalytic subunit. We have undertaken an in-depth survey using the YTH approach to identify proteins, expressed in human testis, capable of interacting specifically with the alternatively splicing isoforms of PP1γ. Among several physiologically interesting proteins, I-2L was identified as a novel putative PP1 binding protein.

Previous studies have attributed an important role to PP1γ2 in mammalian sperm motility. Thus, understanding the molecular basis by which I-2L could be modulating PP1γ2 function in sperm is critical for establishing a physiological role to the PP1γ2-I-2L complex. Furthermore, the contribution of the holoenzyme PP1-I-2L to male (in)fertility will be assessed. The objectives of this study were:

- To analyze the I-2L nucleotide and amino acid sequences using bioinformatics tools.
- To determine the expression of endogenous I-2/I-2L in human sperm and testis.
- To determine the subcellular localization of PP1γ2-(I-2/I-2L) complex in human spermatozoa.
- To optimize the immunoprecipitation assay of I-2/I-2L using a specific anti-I-2 antibody.
- To validate the expression of I-2L *in vivo* by immunoprecipitation from human sperm followed by mass spectrometry analysis.

# 2. Bioinformatics analysis of I-2L

## 2.1. Identification of Inhibitor-2 Like and comparison with Inhibitor-2

There are three different isotypes of protein phosphatase inhibitor-2 (I-2), I-2α1, I-2α2 and I-2β. Two genes encode these three isotypes, with I-2α1 and I-2α2 being isoforms from a single gene, originated from alternative splicing. I-2α2 and I-2β are expressed exclusively in testis, and all three isotypes of I-2 are expressed during sperm maturation (Osawa *et al*., 1996). Here we report the identification of a new protein, termed Inhibitor-2 Like I-2L, from a unique clone (named 48T) (in red, Figure 11) obtained in a YTH screen using PP1γ1 as bait, starting at nucleotide 57 and ending at nucleotide 901 of the sequence NM_206858 in the GenBank database ID (Table 1).

**Table 1:** Inhibitor-2 like (I-2L) clone isolated from the yeast-two hybrid (YTH) screen.

| Clone ID | YTH1 | PP1 BM | chr | Database ID | Insert (bp) | Nº clones |
|---|---|---|---|---|---|---|
| PPP1R2-L<br>I-2L | 48T | KLHY | 5 | NM_206858 | ≈400 | 1 |

Clone 48T (interaction with PP1γ1) was selected for the further study. The occurrence of a consensus PP1 binding motif (PP1 BM) is indicated by the corresponding sequence.

Using the Blast2 algorithm, we aligned the NM_206858 sequence with the human genome and concluded that this sequence is encoded by a gene that is single-exon and maps to chromosome 5, whereas I-2 gene is a five exon gene on chromosome 3. As an intronless gene, I-2L may be evolved into a pseudogene nevertheless it seems to have coding capacity since it came from a cDNA expression library.

By definition, a pseudogene is a gene copy that does not produce a functional, full-length protein. In fact, the human genome is estimated to contain up to 20,000 pseudogenes (Hirotsune *et al*., 2003). In spite of pseudogenes have been defined as nonfunctional sequences of genomic DNA or "junk" DNA (Balakirev and Ayala, 2003), originally derived from functional genes, it is therefore assumed that pseudogenes are not subjected to natural selection and consequently, pseudogene mutations are selectively neutral, being often evolutionary conserved and transcriptionally active. Moreover, pseudogenes may be considered as potogenes, i. e. DNA sequences which have potentiality

to become new genes or acquire new functions (Balakirev and Ayala, 2004). An expressed pseudogene may regulate the mRNA stability of its homologous coding gene (Hirotsune *et al.*, 2003). In literature, there are some examples of expressed pseudogenes. For instance, Sun *et al.* (2008) found that CRIPTO3, a presumed pseudogene, has an open reading frame that differs from Cripto-1 in six amino acids. CRIPTO3 mRNA is the CRIPTO message expressed in many cancer samples, indicating that CRIPTO3 is actually an expressed gene.


**Figure 11:** Nucleotide and amino acid sequences of inhibitor-2 Like (I-2L) (NM_206858). In red is the sequence of the clone 48 (it starts at nt 57 and ends at nt 901). Underlined are the important amino acid sequences involved in PP1 binding. The blue adenine is absent in clone 48T.

Using the ClustalW algorithm we aligned the I-2 and I-2L amino acid sequences, and found that I-2L is 97% identical at the nucleotide level and 95% identical at the amino acid level to I-2. In Figure 12 are highlighted the similarities and differences between this two proteins, being the most preeminent difference the substitution of Thr for Pro at the position 73. This replacement constitutes a very interesting aspect, because of the

importance of this phosphorylation site for the regulation of PP1-I-2 complex. Thr73 can be phosphorylated by several protein kinases such as GSK-3, the cyclin dependent kinase 5 (Cdk5) (Agarwal-Mawal and Paudel, 2001; Mortini *et al.*, 2004), CKII and mitogen-activated protein kinase (MAPK) (Wang *et al.*, 1995). Hence, the absence of the Thr73 in I-2L may be indicative of an alternative mechanism for the inhibitory control of PP1 holoenzyme that rule out the phosphorylation by GSK-3. Another difference is the substitution of Ser by Arg at the position 87, which may alter the regulation by CKII and subsequently, the regulation of PP1 holoenzyme interaction with other proteins such as Nek2 (Fardilha et al., 2004; Wu *et al.*, 2007).

```
I-2   MAASTASHRPIKGILKNKTSTTSSMVASAEQPRGNVDEELSKKSQKWDEMNILATYHPAD 60
I-2L  MAASTASHRPIKGILKNKTSTTSSMVASAEQPRRSVDEELSKKSQKWDEINILATYHPAD 60

I-2   KDYGLMKIDEPSTPYHSMMGDDEDACSDTEATEAMAPDILARKLAAAEGLEPKYRIQEQE 120
I-2L  KGYGLMKIDEPSPPYHSMMGDDEDACRDTETTEAMAPDILAKKLAAAEGLEPKYRIQEQE 120

I-2   SSGEEDSDLSPEEREKKRQFEMKRKLHYNEGLNIKLARQLISKDLHDDDEDEEMLETADG 180
I-2L  SSGEEDSDLSPEEREKKRQFEMRRKLHYNEGLNIKLARQLISKDLHDDDEDEEMLETADG 180

I-2   ESMNTEESNQGSTPSDQQQNKLRSS- 205
I-2L  ESMNTEESNQGSTPSDQQQNKLRSS- 205
```

**Figure 12:** Alignment of predicted amino acid sequences of the I-2 and I-2L. Highlighted residues represent the residues that differ between I-2 and I-2L (in grey). Highlighted in red are represented the most important substitution of Thr73 in I-2 for Pro73 in I-2L.

By searching Prosite and ELM (Puntervoll *et al.*, 2003) for motifs, several phosphorylation sites were found in I-2 and I-2L. CKII phosphorylation sites at the Ser121, Ser122, Ser130 and Thr193 are common to both proteins. However, a new putative CKII phosphorylation site was found at Ser35 in I-2L, whereas the phosphorylation site at Ser87 is absent (Figure 13), denoting that, when these phosphorylation residues are written in the text, we are referring to human I-2 isoform. These results are very intriguing because it has been demonstrated that, in the case of I-2, phosphorylation of Ser86 (rabbit I-2 isoform) by CKII enhances the subsequent phosphorylation at the Thr72 by GSK-3β (Wang *et al.*, 1993; 1995), but does not alter the inhibitory activity of I-2. Furthermore, previews studies showed that Ser120 and Ser121 phosphorylation sites are important for the binding of

GSK-3 (Holmes *et al.*, 1986). There are also three putative phosphorylation sites for the $Ca^{2+}$ and phospholipid-activated protein kinase (PKC) at the Ser7, Ser41 and Ser44 for both I-2 and I-2L. This kinase has been described so far as a regulator of glycogen synthase (Ahmad *et al*., 1984). Moreover, other sequences important for the formation of the PP1-I-2 complex, such the N-terminal SILK-motif ($^{12}$KGILK$^{16}$) (Bollen, 2001; Wakula, 2003), the degenerated RVxF-motif ($^{43}$KSQKW$^{47}$) (Bollen *et al.*, 2010) and the C-terminal FEMKRKLH sequence (Leach *et al.*, 2002) were also identified, which are binding domains to PP1c.

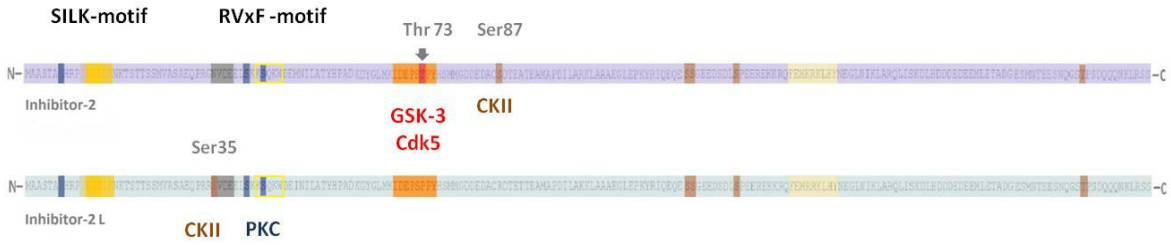


**Figure 13:** Amino acid sequence of inhibitor-2 (I-2) and inhibitor-2L (I-2L). Highlighted residues represent important regulatory sites: PKC phosphorylation site (in blue); CKII phosphorylation site (in brown); GSK-3 and Cdk5 phosphorylation site (in red); KGILK (in yellow); KSQKW (yellow square), EVDE (in grey) and FEMKRKLHY (in beige) are binding domain to PP1c. The region depicted in orange represents the most highly conserved domain of I-2 and I-2L.

Differences in only 9 amino acids (5%) introduce huge differences in terms of signal transduction regulation of these two almost identical proteins I-2/I-2L. This confers completely different functions to the complexes PP1-I-2 and PP1-I-2L, specifically in what concerns to sperm motility (see Figure 9).

### 2.2. Peptide fragments predicted from tryptic digestion

The similarities in terms of nucleotide and amino acid sequence between I-2 and I-2L are enormous, which make it difficult to distinguish between this two proteins by means of molecular and biochemical methods. For instance, the use of antibodies to recognize a specific amino acid sequence of one protein will also recognize the other. Concerning the nucleotide sequence, there are no sufficient differences to allow the design of specific

primers to the corresponding cDNA. For this reason, the strategy adopted pass through the treatment of I-2 and I-2L proteins with a proteolytic enzyme, trypsin, to fragment them, determining then the sizes of fragments by mass spectrometry (MS). We expected that I-2 and I-2L originated unique proteolytic *fingerprint* since the probability of two proteins being cleaved into the same number of fragments, each with the same fragment size is extremely small. Therefore, this was a fine approach to differentiate both proteins and prove the existence of I-2L *in vivo*.

By searching Expasy for potential trypsin cleavage sites, several Arg (R) and Lys (K) residue cleavage sites were found for the I-2 and I-2L peptide sequence. There are 25 putative cleavage sites onto the I-2 peptide sequence and 27 possible cleavage sites onto I-2L peptide sequence (Figure 14). The main difference observed by comparison of the predicted fragments size reside in two peptide fragments with the molecular weight of 2.109 kDa and 1.477 kDa in I-2L instead of 3.625 kDa in I-2, which may be important for distinguish I-2L from I-2 by mass spectrometry. This will be further discussed on chapter 3.

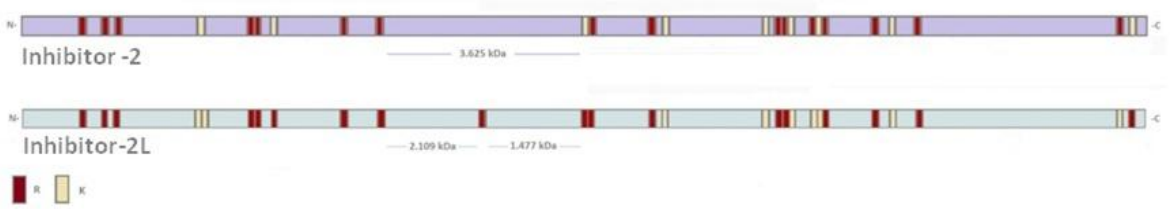


**Figure 14:** Potential cleavage sites of the trypsin protease mapped onto inhibitor-2 (I-2) and inhibitor-2 like (I-2L) protein sequence. The cleavage occurs at the Arginine (R) and Lysine (K) residues at the right side (C-terminal direction of the marked amino acid)**.** Two peptide fragments with the molecular weight of 2.109 kDa and 1.477 kDa in I-2L are predicted instead of 3.625 kDa in I-2.

# 3. Detection and identification of I-2L as a novel putative protein

## 3.1. Expression of endogenous I-2/I-2L in human and rat tissues

### 3.1.1. Introduction

I-2 was first discovered and purified from rabbit skeletal muscle as a protein which could bind to PP1c with a molar ratio of 1:1 and inhibit its activity *in vitro* (Huang and Glinsmann, 1976). I-2 was identified as a heat- and acid- stable protein, ubiquitously expressed in a variety of tissues including skeletal and cardiac muscles, liver, kidney, brain and lung extracts tissues (Park *et al.*, 1994; Roach *et al.*, 1985), testis (Osawa *et al*., 1996) and sperm (Smith *et al*., 1996). Moreover, it has been demonstrated that I-2 inhibitory activity towards PP1 is regulated by phosphorylation at Thr72 (rabbit I-2 isoform) by glycogen synthase kinase-3β (GSK-3β). Sakashita *et al.* (2003) demonstrated by co-immunoprecipitation in COS-7 cells that GSK-3β associates with PP1c-I-2 complex, and phosphorylates I-2 at Thr72 *in vivo*.

I-2 is characterized as a small protein consisting of 204 amino acids, with a predicted molecular weight of 23 kDa and an isoelectric point of 4.64. I-2L was identified from a human testis cDNA library by performing a YTH screen using PP1γ1 as bait, as a clone 95% identical to I-2, with a predicted molecular weight of 23 kDa and an isoelectric point of 4.77. As discussed in Chapter 2, I-2 and I-2L share a remarkable similarity in the full-length sequences, as well in the regions containing the binding domains to PP1, raising the physiological importance of this novel putative PIP.

To analyze the presence of I-2 in rat cortex, heart, liver, kidney and testis extracts, and the presence of I-2/I-2L in human sperm and testis extracts, given that I-2L clone was identified from human testis cDNA library, a specific anti-I-2 antibody was used to analyze the extracts by immunoblotting, thus determining the expression of the endogenous I-2/I-2L. The expression of endogenous PP1γ was also analyzed since I-2L was found in the YTH screen using PP1γ1 as bait. It was used an anti-PP1γ antibody, which recognizes both PP1γ1 (37 kDa) and PP1γ2 (39 kDa) to immunodetect both isoforms.

### 3.1.2. Materials and Methods

#### 3.1.2.1. Human and rat tissues preparation

Rat tissues were obtained from sacrificed animal and immediately frozen on dry ice. Frozen rat tissues were resuspended in boiling 1% SDS and sonicated for 30 sec. Human testis samples were obtained via the kind efforts of Dr. Jorge Oliveira (IPO, Porto), and processed in the same way as the rat tissues.

Human semen samples were collected from healthy adult man donors by masturbation and cryopreservated in liquid nitrogen. The sperm samples had a sperm concentration of $107x10^6$ cells/ml, 80% progressive motility and 16% *in situ* motility, and a volume of 4 ml. These samples were kindly provided by Dr. Vladimiro Silva (FertiCentro, Coimbra). The frozen ejaculated sperm samples were allowed to liquefy at RT before processing. After liquefying, the sperm was extracted from the semen samples using Percoll® (Sigma) density gradient centrifugation according to Dravland and Mortimer (1985), Mortinover (2000) and Dr. Christopher Barrat personal communication (Figure 15).

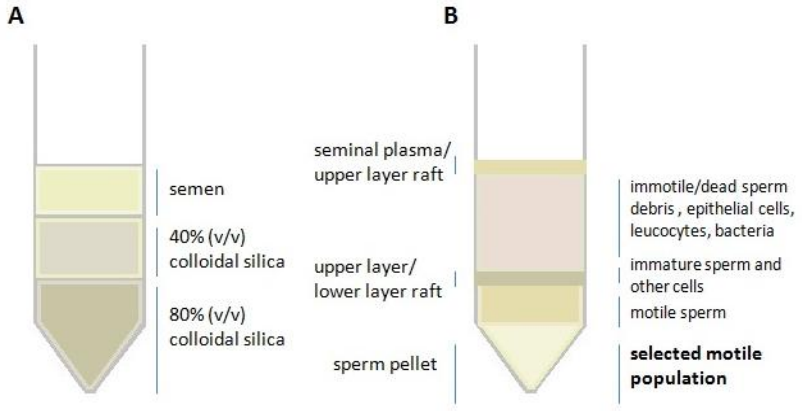


**Figure 15:** Sperm sample selective washing method using density gradient centrifugation with Percoll® 40%/80% buffered in NCB medium. Gradient obtained before **A**| and after **B**| centrifugation (Dr. Christopher Barrat personal communication).

Briefly, semen samples were layered over 40%/80% stepwise Percoll® gradients, buffered with non-capacitating buffer (NCB) (see Table 2 and Appendix), and centrifuged at 500 g for 20 min at RT. The supernatants were discarded and the motile sperm population was selected according to Figure 15. The sperm pellets were pooled and washed twice in 1 ml NCB. The final pellet was resuspended in 150 μl of 1% SDS, and afterward sonicated during 30 sec.

The NCB medium prevents the capacitation of spermatozoa in the ejaculate. The formulation of NCB medium was done according to Dr. Christopher Barrat personal communication, and it differs upon published data (Linhko *et al.*, 2009) in that it contains no bicarbonate ($HCO_3$), to prevent activation of adenylyl cyclase (AC). Also, it has lower concentration of BSA to prevent cholesterol removal, and it has an increased concentration of Hepes to account the reduction of $HCO_3$.

**Table 2:** Formulation of NCB (non-capacitating buffer) medium.

| Components | Concentration (mM) | Amount (g/10 ml) | Volume (ml) |
|---|---|---|---|
| $CaCl_2$ | 1.8 | 0.027 | 1 |
| KCl | 5.4 | 0.040 | 1 |
| $MgSO_4.7H_20$ | 0.8 | 0.020 | 1 |
| NaCl | 116.4 | 0.680 | 1 |
| $NaH_2PO_4$ | 1.0 | 0.016 | 1 |
| D(+)-glucose | 5.6 | 0.100 | 1 |
| Sodium pyruvate | 2.7 | 0.030 | 1 |
| Sodium lactate | 41.8 | 0.468 | 1 |

NCB was buffered with Hepes (25 mM) and adjusted to pH 7.4. 0.3% BSA was added to the final solution.

### 3.1.2.2. Protein assay

Total protein measurements were carried out using Pierce's BCA protein assay kit, following the manufacturer's instructions. The method combines the reduction of $Cu^{2+}$ to $Cu^{+}$ by protein in an alkaline medium (the biuret reaction), with a sensitive colorimetric detection of the $Cu^{+}$ cation using a reagent containing bicinchoninic acid (BCA). The purple-colored reaction product of this assay is formed by the chelation of two molecules

of BCA with one $Cu^{+}$ ion. This water-soluble complex exhibits a strong absorbance at 562 nm that is linear with increasing protein concentration over a working range of 20 μg/ml to 2000 μg/ml. At least duplicate microtubes per sample were prepared to be assayed with 25 μL of each sample plus 25 μL of 1% SDS. Microtubes with standard protein concentrations were prepared as described below (Table 3).

**Table 3:** Standard curve used in the BCA protein assay method

| Standard | BSA (μl) | 10% SDS (μl) | $H_2O$ (μl) | Protein mass (μg) | *WR (ml) |
|---|---|---|---|---|---|
| **$P_0$** | - | 5 | 45 | 0 | 1 |
| **$P_1$** | 1 | 5 | 44 | 2 | 1 |
| **$P_2$** | 2 | 5 | 43 | 4 | 1 |
| **$P_3$** | 5 | 5 | 40 | 10 | 1 |
| **$P_4$** | 10 | 5 | 35 | 20 | 1 |
| **$P_5$** | 20 | 5 | 25 | 40 | 1 |
| **$P_6$** | 40 | 5 | 5 | 80 | 1 |

*WR (working reagent)

The BSA stock solution used had a concentration of 2 mg/ml. The Working Reagent (WR) was prepared by mixing BCA reagent A with BCA reagent B in the proportion of 50:1. Then, 1 ml of WR was added to each microtube (standards and samples) and the microtubes were incubated at 37 ºC for 30 min. Once the tubes cooled to RT the absorbance was measured at 562 nm. A standard curve was obtained by plotting BSA standard absorbance *vs* BSA concentration, and used to determine the total protein concentration of each sample.

### 3.1.2.3. SDS-PAGE

In SDS polyacrylamide gel electrophoresis (SDS-PAGE) separations were carried out using well established methods (Sambrook *et al.*, 1989). The percentage and size of the gel used depended on the molecular weight of the proteins being separated in the gel (Table 4). In the time course analysis, to visualize the I-2 and PP1γ, with an apparent molecular weight around 32 kDa and 37 kDa, respectively, a 10% acrylamide gel was used.

**Table 4:** Composition of the running and stacking gels for SDS-PAGE (*mini gels*).

| Components | Running gel (10%) | Stacking gel (3.5%) |
|---|---|---|
| **Water** | 4.2 ml | 3.3 ml |
| **30% Acryl/8% Bisacryl.** | 3.3 ml | 0.6 ml |
| **4x LGB** | 2.5 ml | --- |
| **5x UGB** | --- | 1.0 ml |
| **SDS 10%** | --- | 50 µl |
| **10% APS** | 50 µl | 50 µl |
| **TEMED** | 5 µl | 5 µl |

The 10% running gel was prepared by sequentially adding the components indicated on Table 4 (APS and TEMED were added last, as they initiate the polymerizing process). The solution was pipetted down the spacer into the gel sandwich, leaving some space for the stacking gel. Then, the water was carefully added to cover the top of the gel and the gel was allowed to polymerize for 1 hr. The stacking gel was prepared according to Table 4. The water was poured out and the stacking gel was added to the sandwich; a comb was inserted and the gel was allowed to polymerize for 30 min.

After the gel polymerization, the combs were removed, and the wells filled with running buffer. The samples previously prepared were carefully applied into the wells. The gel run for 2 hr at 100 V until bromophenol blue from the LB reached the bottom.

### 3.1.2.4. Immunoblotting

For immunoblotting, the tank transfer system was used as follows: 3MM blotter paper was cut to fit the transfer cassette and a nitrocellulose membrane of the gel size was also cut. The gel was removed from the electrophoresis device and the stacking gel removed and discarded. The transfer sandwich was assembled under transfer buffer to avoid trapping air bubbles. The cassette was placed in the transfer device filled with transfer buffer. Transfer was allowed to proceed for 2 hr at 200 mA. Afterwards, the transfer cassettes were disassembled; the membrane carefully removed and allowed to air dry prior to further manipulations.

The immunodetection was carried by enhanced chemiluminescence (ECL). ECL$^{TM}$ (Amersham) is a light emitting non-radioactive method for the detection of immobilized antigens, conjugated directly or indirectly with horseradish peroxidase-labelled antibodies.

In order to visualize the proteins, the blots were probed with a polyclonal anti-I-2 antibody (see section 3.1.2.5), which recognizes the I-2/I-2L proteins. The membranes were soaked in 1xTBS for 5 min. Non-specific binding sites were blocked by immersing the membrane in 3% low fat milk in 1xTBST for 1 hr. After washing with 1xTBST, the membrane was incubated with a solution of the primary antibody (anti-I-2; 1:100), diluted in 3% low fat milk in 1xTBST for 2 hr with shaking. After three washes of 10 min each in 1xTBST, the membrane was incubated with a solution of the anti-sheep secondary antibody diluted for ECL (1:1000) in 3% low fat milk in 1xTBST for 2 hr with shaking. The membrane was then washed 3 times with 1xTBST for 10 min. Subsequently, the membrane was incubated for 1 min with the ECL detection solution (a mixture of equal volumes of solution 1 and solution 2 from the ECL kit (Amersham), approximately 0.125 ml/cm$^2$ membrane). Inside the dark room, the membrane was gently wrapped with cling-film, eliminating all air bubbles and placed in a film cassette and an autoradiography film (XAR-5 film, KODAK) was placed on the top. The cassette was closed and the blot exposed for 10 min. The film was then removed and developed in a developing solution, washed in water and fixed in fixing solution.

To immunodetect PP1γ, the same membrane was washed three times with 1xTBS-T during 30 minutes and then blocked in 3% low fat milk in 1xTBST for 1 hr before incubate the membrane with a solution of the primary antibody (CBC3C anti-PP1γ; 1:1000), diluted in 3% low fat milk in 1xTBST, for 2 hr with shaking. After this period, three washes of 10 min each in 1xTBST were done, and the membrane was next incubated with a solution of the anti-rabbit secondary antibody diluted for ECL (1:5000) in 3% low fat milk in 1xTBST for 2 hr with shaking. This membrane was prepared for ECL detection following the procedure described before.

As a control, this membrane was also incubated with anti-β-tubulin antibody, to determine if the quantity of protein loaded into the gel was equal for all samples. The same membrane was washed three times during 10 min with 1xTBST, blocked in 3% low fat milk in 1xTBST for 1 hr before incubate the membrane with a solution of the primary antibody (anti-β-tubulin; 1:500), diluted in 3% low fat milk in 1xTBST for 2 hr with shaking. After this period, three washes of 10 min each in 1xTBST were done, and the membrane was then incubated with a solution of the anti-mouse fluorescein isothiocyanate (FITC) conjugated antibody (1:1000) in 3% low fat milk in 1xTBST for 2 hr with shaking. The membrane was then washed twice with 1xTBST for 10 min and 1xTBS for 1 min and the membrane observed in a Odyssey® infrared imaging system version 2.1 (LI-COR Biosciences, USA).

#### 3.1.2.5. Anti-I-2 antibody

The anti-I-2 antibody was previously purified in our laboratory by Wenjuan Wu, by affinity column purification of antibody-containing sheep serum, kingly provided by Dr. David Brautigan. As the concentration of the antibody was too low (0.04 mg/ml), the anti-I-2 antibody was then concentrated using a Centripep® (Millipore) centrifugal filter device following the manufacture's procedure.

The concentration of anti-I-2 antibody was measured at 280 nm (1.4 OD=1 mg/ml) and corresponded to 0.5 mg/ml. Afterwards, the antibody was diluted (1:100) in 3% low fat milk in 1xTBST and an immunoblot (see section 3.1.3.1) was performed using His-tagged I-2 that was expressed in *Escherichia coli* and purified in our laboratory by Ana Vintém.

### 3.1.3. Results

#### 3.1.3.1. Detection of purified His-tagged I-2 with anti-I-2 antibody

In order to test the polyclonal anti-I-2 antibody (0.5 mg/ml) affinity to I-2, an immunoblot was performed using different amounts of purified I-2-His. As shown in Figure 16, a dilution (1:100) of anti-I-2 antibody was used to recognize 100 ng, 10 ng, 1 ng and 0.1 ng of purified I-2 His, being the fusion protein identified at 37 kDa. Thus, this anti-I-2 antibody (1:100) was used for further experiments.

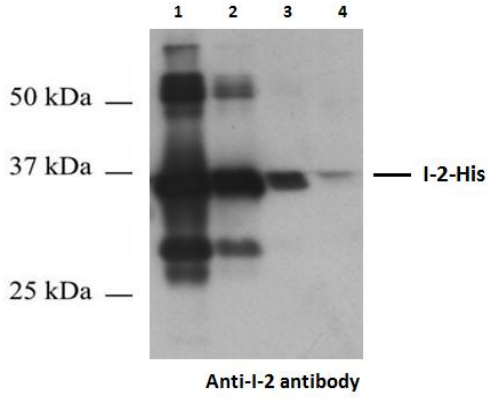


**Figure 16:** Immunoblot analysis of purified I-2-His (1-4) using the polyclonal anti-I-2 antibody (1:100). 1, I-2-His (100 ng); 2, I-2-His (10 ng); 3, I-2-His (1 ng); 4, I-2-His (0.1 ng).

#### 3.1.3.2. Tissue distribution of I-2/I-2L proteins

The tissue distribution of I-2 and I-2/I-2L was evaluated by immunoblot analysis of different rat tissues, and human testis and sperm. From Figure 17a it was evident that I-2/I-2L proteins were present in human and rat testis and in human sperm. Besides these tissues, I-2 was also expressed in rat cortex, heart, kidney and liver, but it seems to be less expressed in liver. I-2/I-2L, intrinsically unstructured proteins (IUPs), run in the SDS-PAGE gel with a higher molecular weight (32 kDa) than the predicted (23 kDa).

Concomitantly, the tissue distribution of PP1γ is shown in Figure 17b, since PP1γ isoforms interact with I-2 in several tissues. It was reported before that the levels of PP1γ2 activity are higher in testis and sperm allied with the role of I-2 in sperm maturation.

Furthermore, I-2L was shown to putatively interact with PP1γ1 isoform in testis (see Chapter 2). Anti-PP1γ antibody was used to immunodetect both PP1γ1 and PP1γ2 in several tissues. In rat tissues, the levels of expression for these PP1γ isoforms were higher for cortex, kidney and testis, and lower for heart and liver. It is also apparent that the amount of PP1γ in testis is higher in rat testis than in human testis. Evaluating the levels of expression in human sperm and testis, it is evident that sperm contains more PP1γ than testis.

These results are intriguing when the levels of expression of I-2/I-2L and PP1γ isoforms are compared, since these results indicated that, in testis, low expression of PP1γ isoforms correlates with high levels of expression of I-2/I-2L, and high expression of PP1γ isoforms, mainly PP1γ2, correlates with lower expression of I-2/I-2L. These curious results will be discussed bellow (see section 3.1.4).

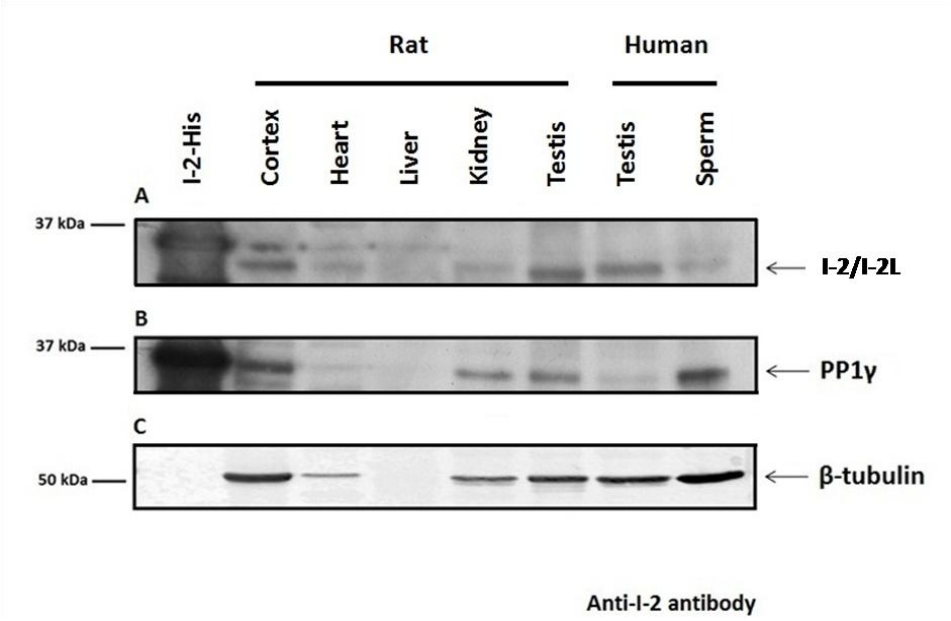


**Figure 17:** I-2 and I-2/I-2L tissues screen. **A**| A multiple tissue screening (25 µg) of I-2 was performed using anti-I-2 (1:100) antibody, and purified I-2-His (50 ng) was used as positive control. The predicted molecular weight of I-2/I-2L is 23 kDa. **B**| The same membrane was incubated with a C-terminus anti-PP1γ antibody (1:1000) to perform a PP1γ tissue screening. The molecular weight of PP1γ1 and PP1γ2 is 37 kDa and 39 kDa, respectively. **C**| The β-tubulin was used as control. I-2/I-2L run in the SDS-PAGE gel with an apparent molecular weight of 32 kDa.

### 3.1.4. Discussion

I-2L was identified in an YTH screen, using PP1γ1 as bait and a human testis cDNA library, as a putative PP1γ1 interactor, very similar to I-2, an ancient and highly conserved inhibitor of PP1. Subsequently, a bioinformatics analysis of the encoded protein revealed several physiologically relevant features of the protein (see Chapter 2).

Further, we performed an immunoblot analysis of several rat tissues, and human testis and sperm. These results showed that I-2/I-2L were present in most of the analyzed tissues (Figure 17). Expression of I-2/I-2L was observed in human testis and sperm. These results suggested that I-2/I-2L have an important role in the inhibition of PP1γ2, which is also present, as indicated by the results, in sperm. In contrast, low levels of expression of I-2/I-2L and PP1γ isoforms were detected in rat liver.

Several studies indicated that I-2 has an important physiological role in several tissues. For instance, Terry-Lorenzo *et al*. (2002) have shown from rat brain extracts that I-2 binds to PP1 and several other binding proteins forming a multiprotein complex. For example PP1-I-2 binds to actin-binding proteins, neurabin I and neurabin II/spinophilin, which are neuronal actin-binding proteins that targeted PP1 to F-actin and regulate cell morphology. I-2 was also identified in cardiomyocytes, as reported in several studies (Gupta *et al.*, 2005; Yamada *et al.*, 2006). Studies *in vivo* with mice overexpressing I-2 demonstrated that PP1 activity is decreased concomitantly with the enhanced contractility in heart, suggesting that I-2 improves the cardiac performance (Kirchhefer *et al*., 2005). I-2 has also been previously identified to be largely expressed in rat kidney extracts, accordantly with the earlier reports with other mammalian kidney extracts (Roach *et al*., 1985). Concerning to the expression of I-2 in rat liver, the results indicated that I-2 has lower expression in liver, contrary to the results reported by Roach *et al*. (1985) and by Park *et al.* (1994) with rabbit liver extracts. In addition, previous results from our laboratory have demonstrated that I-2 and PP1γ1 isoforms have low expression in rat liver extracts (unpublished results).

The presence of I-2/I-2L in rat and human testis and in human sperm was confirmed by immunoblotting analysis, as well as the presence of PP1γ isoforms, specifically PP1γ2. Indeed, I-2/I-2L and PP1γ2 are expressed in rat testis, and in human testis and sperm. The

expression of I-2 and PP1γ2 in germ tissues has been documented previously (Chakrabarti *et al.*, 2007; Osawa *et al.*, 1996). PP1γ2 is expressed during germ cell differentiation in testis and during spermatozoa maturation, and its activity is related with I-2-like activity that was reported to exist in human sperm (Chakrabarti *et al.*, 2007; Huang and Vijayaraghavan, 2004; Vijayaraghavan *et al.*, 1996). Our results indicated that the ratio PP1γ2-(I-2/I-2L) is different in human testis and sperm probably meaning differences in the complex regulation. Moreover, sperm samples with different motility parameters (unpublished results) also present different PP1γ2-(I-2/I-2L) ratios. These ratios might serve as a diagnostic tool to male infertility.

## 3.2. Co-localization of I-2/I-2L with PP1γ2 isoform in human spermatozoa

### 3.2.1. Introduction

In order to determine if PP1γ2 and I-2/I-2L co-localize in human sperm cells, subcellular localization studies were carried out. Human semen has a corpuscular and liquid component. The corpuscular compartments are spermatozoa, immature germ cells, sloughed-off epithelial cells from the seminiferous tubules, spermatophages, cytoplasmic droplets and leukocytes. Cells of the testis, epididymis and accessory glands secrete the liquid components of the seminal plasma (De Jonge and Barratt, 2006). Ejaculated spermatozoa are motile but they need to undergo capacitation in the female genital tract before they can fertilize an oocyte (Turner, 2003). The epididymal sperm maturation and development of sperm motility in the epididymal tract involves changes in PP1γ2 activity, which is the major PP1γ isoform in sperm (Huang and Vijayaraghavan, 2004). *In vitro* studies indicated that PP1γ2 is active in bovine, monkey, macaque and human caput spermatozoa and its activity decreases in caudal spermatozoa (Smith *et al*., 1996; 1999). This regulation is triggered by I-2/I-2L that is a highly expressed inhibitor in human sperm, as demonstrated before (section 3.1.3.2).

Thus, to allow the analysis of the endogenous I-2/I-2L expression and subcellular distribution in human spermatozoa and its co-localization with endogenous PP1γ2 by immunocytochemistry, specific antibodies were used which recognizes specifically I-2/I-2L and PP1γ2 isoform.

### 3.2.2. Material and Methods

#### 3.2.2.1. Immunocytochemistry procedure

Sperm cells were prepared by selective washing using Percoll® gradient, following the protocol described previously. To the final pellet was added 300 µl of a solution containing NCB medium (Table 2) in 0.3% BSA. The human semen sample was kingly provided by Dr. Vladimiro Silva (FertiCentro, Coimbra), obtained from a healthy adult man volunteer by masturbation and cryopreserved in liquid nitrogen. The sperm sample had a sperm concentration of $36x10^6$ cells/ml, a 68% progressive motility and 4% *in situ* motility, and a volume of 2 ml.

An aliquot of sperm cells (25 µl) was placed onto a glass coverslip pre-coated with 100 µg/ml poly-L-ornithine, and dried at RT, in a six well plate containing one coverslip per well. To each well was gently added 1 ml of 4% paraformaldehyde in PBS and left to stand for 10 min. Subsequently, sperm cells were washed twice with 1 ml 1xPBS for 10 min. For sperm cells permeabilization, 1 ml of 1:1 methanol/acetone solution was added for 2 min and then washed twice with 1 ml 1xPBS for 10 min. The cells were blocked out for 1 hr with 3% BSA in 1xPBS, and then were incubated with primary antibody for 2 hours at RT. After three washes with 1xPBS, the secondary antibody was added and the coverslips incubated for 2 hr. Finally, three washes with 1xPBS were performed and coverslips were mounted on microscope glass slides with one drop of anti-fading reagent containing DAPI for nucleic acid staining (Vectashield, Vector Laboratories). Photographies were acquired using an epifluorescence microscope equipped with appropriate software (Olympus IX81).

The primary antibodies used were the rabbit polyclonal anti-PP1γ2 (G502; 1:1000) and the sheep polyclonal anti-I-2 antibody (1:100). The secondary antibodies used were the anti-sheep fluorescein isothiocyanate (FITC) conjugated antibody (1:50) and the anti-rabbit Texas Red conjugated antibody (1:300). The antibodies were diluted in 3% BSA in 1xPBS. The antibodies were added subsequently, according to the description in Figure 18.

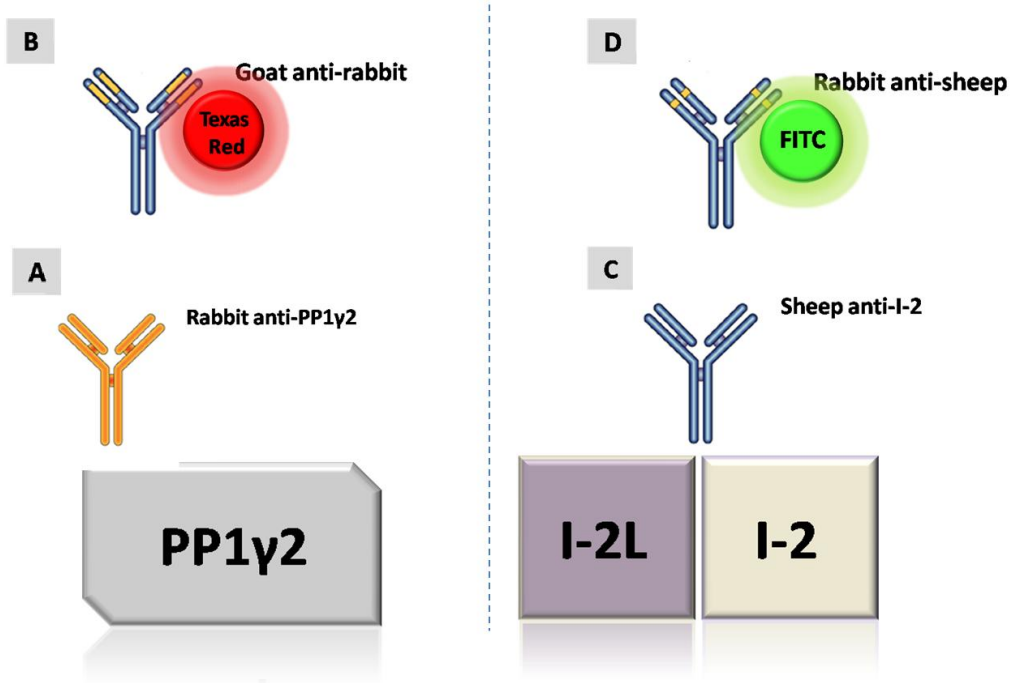


**Figure 18:** Immunocytochemistry procedure for subcellular localization of PP1γ2 and I-2/I-2L in human sperm. The primary and secondary antibodies used were added to the sperm sample sequentially. **A**| The anti-PP1γ2 antibody (G502; 1:1000) was first added to the sperm sample. **B**| The secondary anti-rabbit Texas Red conjugated antibody (1:300) was added after the anti-PP1γ2 antibody. The dashed blue line represents the washing procedure before the incubation with the anti-I-2 antibody. **C**| The anti-I-2 antibody (1:100) was thirdly added to the sperm sample after the washing procedure. **D**| The secondary anti-sheep fluorescein isothiocyanate (FITC) conjugated antibody (1:50) was added after the anti-I-2 antibody.

### 3.2.3. Results

Immunofluorescence was used to localize I-2/I-2L and PP1γ2 within human spermatozoa. As seen in Figure 19a, in morphological normal spermatozoa, PP1γ2 and I-2/I-2L co-localize at the principal-piece and middle-piece of flagellum and at the equatorial and postacrosomal segment of the head region. The staining appears to be specific since there was no fluorescence observed when the primary antibodies were omitted (data not shown).

Co-localization of I-2/I-2L and PP1γ2 in abnormal human spermatozoa was also evaluated (Figure 19b-e). In abnormal tail spermatozoa (Figure 19b), co-localization of I-2/I-2L with PP1γ2 was detected at the middle- and principal- piece of flagellum and at the postacrosomal region of the spermatozoa head. Interestingly, the percentage of co-localization seems lower when compared to morphological normal spermatozoa. In middle-piece abnormal spermatozoa (Figure 19c), co-localization of I-2/I-2L with PP1γ2 was detected in the entire length of the flagellum and in the equatorial region of the spermatozoa head. Comparatively, in abnormal head spermatozoa (Figure19d), I-2/I-2L co-localize with PP1γ2 in the principal-piece and middle-piece of flagellum, and in the equatorial and postacrosomal segment of the head region, resembling normal spermatozoa (Figure 19a). More interestingly, was the staining in spermatozoa with multiple abnormalities (Figure 19e). I-2/I-2L was absent from the tail. PP1γ2 and I-2/I-2L staining in the head was diffuse and co-localize.

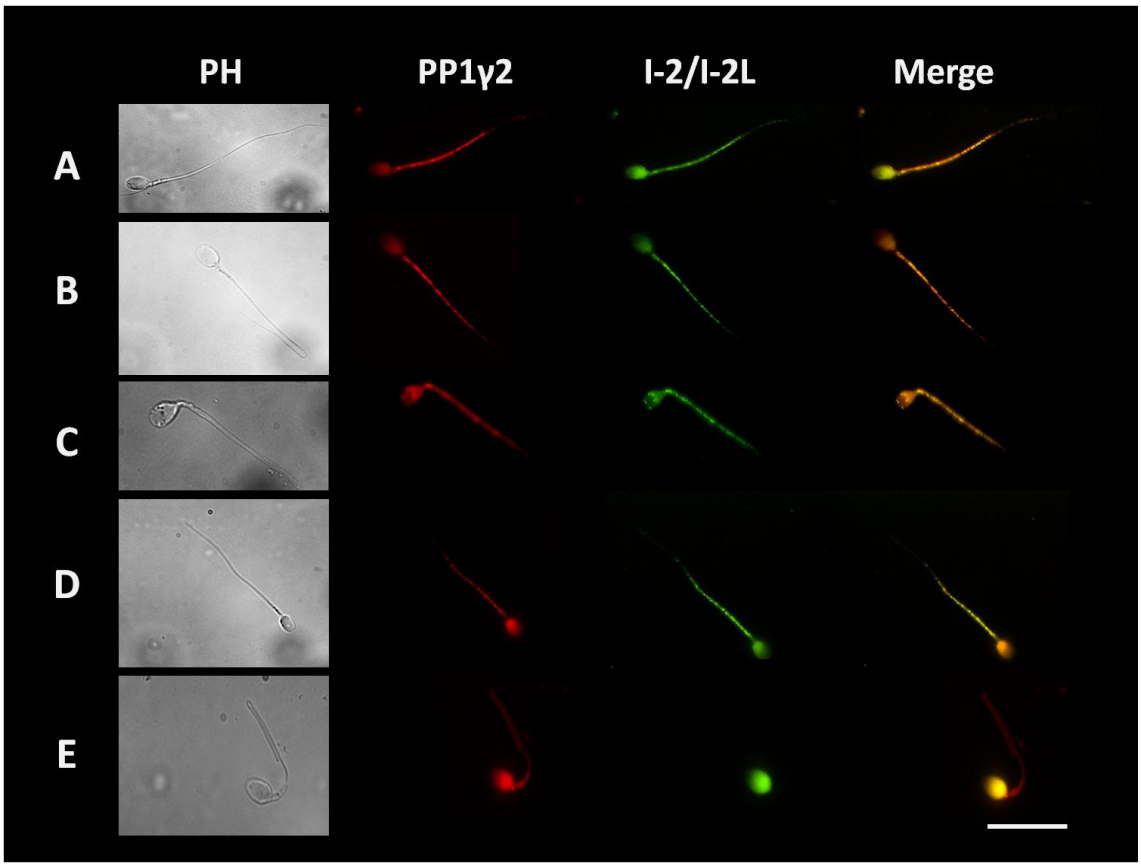


**Figure 19:** Co-localization of PP1γ2 and I-2/I-2L in morphologically normal and abnormal spermatozoa. Human spermatozoa were labeled with anti-PP1γ2 and anti-I-2 antibodies, and specific secondary antibodies conjugated with Texas Red and FITC fluorophores, respectively. **A**| Normal spermatozoa. **B**| Abnormal tail spermatozoa. **C**| Abnormal middle-piece spermatozoa. **D**| Abnormal head spermatozoa. **E**| Multiple abnormalities spermatozoa. Phase contrast (PH). Scale bar = 20 µm.

### 3.2.4. Discussion

PP1γ1 and PP1γ2 isoforms originated from alternative splice of the *PP1γ* gene are differentially expressed. Unlike PP1γ2 that is sperm- and testis- enriched, PP1γ1 is expressed in various tissues (da Cruz e Silva *et al.*, 1995; Huang and Vijayaraghavan, 2004; Smith *et al.*, 1996). Among others, I-2-Like activity is an important inhibitor of PP1γ2 activity in ejaculated human sperm (Smith *et al.*, 1999). Through immunocytochemitry, using an anti-I-2 antibody, which recognizes I-2/I-2L proteins, we showed that in human sperm, PP1γ2 co-localizes endogenously with I-2/I-2L, and those co-localize in the sperm tail, specifically in the middle-piece and the principal-piece (Figure 19), consistent with the regulatory role for PP1γ2 and I-2/I-2L in the control of sperm motility. Co-localization also occurs in the spermatozoa postacrosomal and equatorial segment of the head region, suggesting a role in the acrosome reaction. The expression of PP1γ2 during cell differentiation in testis has been well documented (Chakrabarti *et al*., 2007; Osawa *et al*., 1996), and the PP1 involvement in the onset of hyperactivated motility and the acrosome reaction was also reported (Breitbart, 2002; Küpker *et al.*, 1998; Si and Okuno, 1999; Turner, 2003).

PP1γ2 co-localization with I-2/I-2L in spermatozoa flagellum may also indicate the importance of PP1γ2-(I-2/I-2L) complex in sperm morphogenesis, in addition to its role in motility. Chakrabarti and collaborators (2007) demonstrated *in vivo*, using *Ppp1cc*-null mice, that PP1γ2 is involved in sperm tail morphogenesis, and that the absence of this protein lead to the reduction in the levels of postmeiotic proteins such as AKAP4 and sds22 (Huang *et al.*, 2002), that regulate PP1γ2, and are associated with sperm tail development and function. The distribution pattern of PP1γ2 and I-2/I-2L in abnormal spermatozoa was very intriguing when compared to normal spermatozoa, where PP1γ2 co-localizes with I-2/I-2L only in the middle- and principal- piece of flagellum compared to the previous. Accordingly, testicular sperm tails from *Ppp1cc*-null mice demonstrated a variety of abnormalities in both middle and principal pieces, suggesting some deregulation of PP1γ2-(I-2/I-2L) complex in sperm differentiation and morphogenesis (Chakrabarti *et al*., 2007). Additionally, it has been demonstrated that PP1γ2 and I-2 expression levels increase significantly during spermiogenesis (Chakrabarti *et al*., 2007; Osawa *et al*., 1996).

This is another indication of the importance of PP1γ2-(I-2/I-2L) complex in sperm development.

The results presented in this chapter indicated that the role of PP1γ2-(I-2/I-2L) complex in spermatozoa morphogenesis and motility is possibly related with the arrangement of the flagellum. Chakrabarti *et al*. (2007) demonstrated that tail abnormalities in *Ppp1cc*-null sperm include middle-pieces that had disorganized mitochondrial sheaths or were thinner than principal pieces due to the absence of mitochondrial sheaths. Wang and Brautigan (2008) demonstrated the importance of I-2 in the acetylation of microtubules that make up the axoneme contributing for the stability of the structure, in I-2 knockdown cells by siRNA. PP1 has been localized in *Chlamydomonas* axonemal central pair apparatus (Yang *et al.*, 2000). Several evidences support a role for PP1γ2-(I-2/I-2L) complex in the regulation of sperm motility by being involved in sperm tail dynamics (Figure 20). Indeed, PP1γ2 co-localizes with I-2/I-2L in equatorial and postacrosomal segment of the head, middle- and principal- piece of flagella (in grey, Figure 20) in morphologically normal spermatozoa. When defects are present, PP1γ2-(I-2/I-2L) expression is altered and presumably also the complex functions. In the more extreme case, the spermatozoa with multiple abnormalities, I-2/I-2L are no longer expressed in the tail probably meaning that PP1γ2 is not being inhibited and consequently active. This will lead to an immotile sperm cell (Vijayaraghavan *et al*., 1996; 2000).

Here we propose a putative diagnostic tool to compare at the molecular level morphologically different sperm cells based on the co-expression of PP1γ2-(I-2/I-2L).

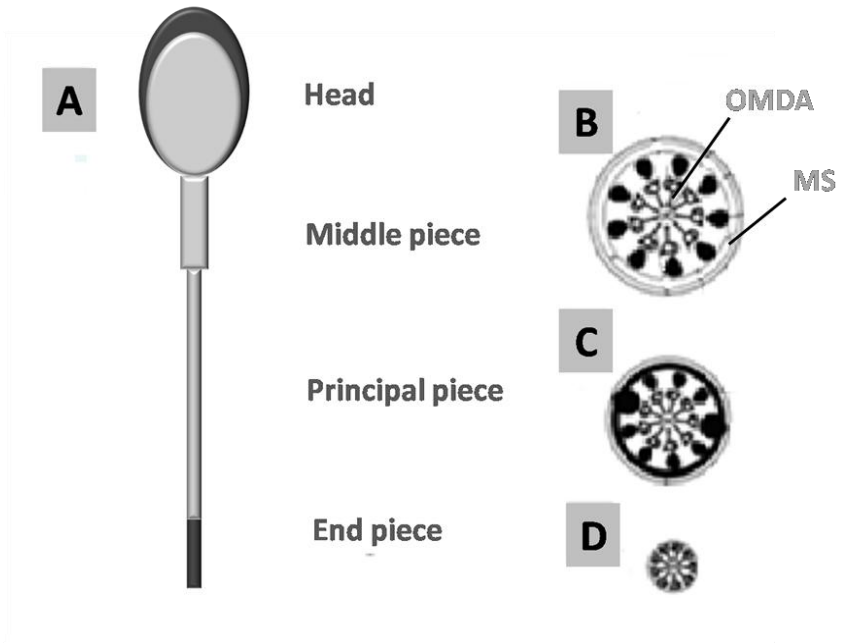


**Figure 20:** Schematic representation of the mammalian spermatozoa and the ultra-structure of flagellum **A**| Mammalian sperm is composed of head divided into acrosome, equatorial and postacrosomal regions, and flagella is divided into middle-piece, principal-piece and end-piece. In grey are represented the regions where PP1γ2 co-localize with I-2/I-2L (equatorial and postacrosomal segment of the head, middle- and principal-piece of flagellum). **B**|-**D**| Schematic cross-section through a representative segment of flagellum, highlighting the middle-piece **B**|, principal-piece **C**|, end-piece **D**|. Along the flagellum, the axonemal components (OMDA) arranged 9+2 (9 outer microtubules doublets and the central pair of microtubules doublets) are unchanged but the mitochondrial sheath (MS) is only present in the middle-piece region (adapted from Turner, 2003).

## 3.3. Immunoprecipitation of I-2/I-2L and mass spectrometry analysis

### 3.3.1. Introduction

Through immunoblot analysis (see section 3.1.3.2) we showed that PP1γ2 and I-2/I-2L are expressed in human testis and sperm, and through immunocytochemistry (see section 3.2.3) we showed that in human sperm PP1γ2 co-localizes endogenously with I-2/I-2L in sperm tail. Thus, the results are consistent with the occurrence of I-2/I-2L in sperm, previously described, but did not allow us to reach any conclusions regarding the occurrence of I-2L protein, since the methods used employed antibodies, specifically anti-I-2 antibody, that may recognize both I-2/I-2L proteins. Certainly, if I-2L is expressed, it interacts endogenously with PP1γ2 in human spermatozoa, but this interaction does not occur in the terminal end of flagellum and the acrosomal region of the head, as suggested by previous results (Figure 19 and 20) because the results have shown the presence of I-2/I-2L in the equatorial and postacrosomal segments of the head, and the middle- and principal pieces- of the flagellum.

To analyze if I-2/I-2L and PP1γ2 interacts, several experiments were previously performed in our laboratory by Ana Vintém and Wenjuan Wu. However these results do not guarantee the existence *in vivo* of I-2L protein. Nevertheless, the *in vitro* binding of purified I-2L with both PP1γ isoforms was confirmed by overlay. Also Co-IP from human sperm confirmed PP1γ2 and I-2/I-2L interaction (data not shown).

With the proposal of confirming that I-2L is expressed and interacts with PP1γ2 in human sperm, and address the physiological relevance *in vivo* of PP1γ2-I-2L interaction, we attempted to immunoprecipitate I-2/I-2L from human sperm extracts, to analyze the immunoprecipitates (IP) by mass spectrometry (MS), thus trying to identify a specific peptide profile (Lodge *et al.*, 2007). To that end, the immunoprecipitation with anti-I-2 antibody followed by immunoblot analysis of the IP and in-gel extraction of the band corresponding to I-2/I-2L was performed. Optimization of immunoprecipitation protocol for the anti-I-2 antibody and target proteins (I-2/I-2L) was done in order to obtain a successful I-2/I-2L protein capture due to the fact that some antibodies may show a reduced antigen-binding efficiency for immunoprecipitation assay (Sambrook *et al.*, 1989).

### 3.3.2. Material and Methods

#### 3.3.2.1. Optimization of immunoprecipitation protocol

Purified I-2-His (100 ng) was pre-incubated with 2 µl of anti-I-2 antibody (0.5 mg/ml) in 500 µl of 3% BSA in 1xPBS buffer for 1h at 4 ºC with rotation. After this period, 50 µl of Protein G Sepharose slurry (Amersham) was added, and the mixture was incubated overnight at 4 ºC with agitation. Protein G Sepharose slurry was previously prepared by centrifugation during 1 min at 4 ºC at 10.000 g and by washing the pellet three times with 3% BSA in 1xPBS buffer at 4 ºC.

After centrifuging the sample for 1 min at 4 ºC at 10.000 g, the supernatant was removed and the pellet washed twice for 10 min with 500 µl of 3% BSA in 1% PBS buffer. The pellet was resuspended in 25 µl of electrophoresis buffer (loading buffer for SDS-PAGE) and before loading, the IgG of the sample was eluted from protein G by two alternative methods: by the addition of 0.1 M glycine buffer, pH 3.0 as elution buffer followed by the neutralization of the sample with 1M Tris-HCl, pH 9.0, or by heating the sample for 3 min at 90 ºC. The sample was briefly centrifuged to pellet the Sepharose beads and the supernatant applied to the gel.

For the Dynabeads® Protein G (Invitrogen) protocol, 2 µl of I-2 antibody (0.5 mg/ml) diluted in 200 µl 3% BSA in 1xPBS buffer was directly added to 100 µl Dynabeads (3.0 mg), previously prepared by placing the tube containing the Dynabeads on the magnet (Dynal MPC®) to separate the beads from the supplied solution, and by washing the pellet twice with 200 µl of 3% BSA in 1xPBS buffer. The mixture was incubated with rotation during 1 h at 4 ºC, and the tube was then placed on the magnet and the supernatant removed. The Dynabeads-Ab complex was resuspended in 200 µl 3% BSA in 1xPBS buffer, and 100 ng of purified I-2-His were added and incubated overnight with rotation at 4 ºC to allow the binding to the Dynabeads-Ab complex. After this period, the tube was placed on the magnet, the supernatant was removed and the pellet washed three times using 200 µl 3% BSA in 1xPBS buffer for each wash. The pellet was resuspended in 100 µl 3% BSA in 1xPBS buffer and transferred to a clean tube. Finally, the tube was placed on the magnet, the supernatant was removed and the denaturing elution was

performed by the addition of 1/4 volume of electrophoresis buffer (loading buffer for SDS-PAGE) and before loading onto the gel, the IgG of the sample was eluted from protein G by heat for 10 min at 70 ºC.

### 3.3.2.2. Immunoprecipitation procedure

After selective washing of the semen sample by Percoll® centrifugation gradient, following the procedure described in section 3.1.2.1, the pellet containing motile spermatozoa was resuspended in 500 µl of 1xPBS containing a protease inhibitor cocktail (see Appendix). The sample was sonicated for 5 sec three times, intercalating the samples in order not to over-heat them. After BCA protein quantification described before in section 3.1.2.1 mass normalized lysates were pre-cleared with 20 µl of Dynabeads® Protein G (Invitrogen), previously prepared in 100 µl of 1% PBS in 3% BSA, for 1 hr at 4ºC with agitation. At the same time, the remaining volume (80 µl) of Dynabeads® Protein G (Invitrogen) were also pre-incubated with 2 µl of anti-I-2 antibody (0.5 mg/ml), during 1 hr at 4 ºC with rotation. The Dynabeads® Protein G used was previously prepared taking into account the protocol for the optimized immunoprecipitation (see section 3.3.2.1). After incubation, the tubes containing the samples were placed on the magnet (Dynal MPC®) and processed as follows: the supernatant from the tube containing the Dynabeads® Protein G-Ab complex was discarded and the supernatant from the pre-clearance was added to the prior tube. This mixture was then incubated overnight with shaking at 4 ºC. Afterward, the tube containing the mixture was placed on the magnet and washed three times with 1xPBS in 3% BSA for 10 minutes with agitation at 4 ºC. Before the last wash, the mixture was transferred into a new tube, and after the last wash the supernatant was discarded and the beads were resuspended in 100 µl of loading buffer/1% SDS and boiled for 10 minutes at 70 ºC. The lysates from the same semen sample were also collected (25 µg) and the appropriated volume of 10% SDS was added to obtain a final concentration of 1% SDS. Then, they were boiled for 10 min and frozen.

Immunoprecipitates and lysates were separated by 10% SDS-PAGE. The lysates and 40 µl of the immunoprecipitate were loaded in one of two gels, and the remaining immunoprecipitate (60 µl) was loaded in the other gel. The first gel was transferred to a

nitrocellulose membrane that was then incubated with anti-I-2 antibody (1:100) and the second gel was stained with Coomassie blue colloidal (see section 3.3.2.3).

#### 3.3.2.3. Coomassie blue colloidal staining and I-2/I-2L in-gel extraction

Coomassie blue colloidal staining is based on non-specific binding of Coomassie blue dye to proteins. Separated proteins are simultaneously fixed and staining in the gel and then distained to remove the background prior to drying. The proteins are detected as blue bands on a clear background.

The gel containing the immunoprecipitated was fixed by placing it in the fixation solution during 1 hour. After the gel was fixed, the gel was washed with distillated water and then transferred to the Coomassie blue colloidal staining solution and stained for 1 hr with agitation. After the gel was stained, the gel was washed with distillated water and afterwards distained with distain solution for 1 hr. After the first hour of distaining, fresh distaining solution was added and the gel was distained overnight.

In view of the fact that I-2 and I-2L were immunoprecipitated together, because anti-I-2 antibody recognizes both proteins, a single band was stained corresponding to I-2/I-2L proteins with the molecular weight of 32 kDa. This single band was extracted directly from the gel using one spatula, and the sample was stored at -80 ºC for further mass spectrometry analysis.

### 3.3.3. Results

In order to confirm the expression of I-2/I-2L *in vivo*, immunoprecipitation assay was carried out using human sperm extracts. Immunoprecipitation was performed using anti-I-2 antibody. Firstly, the immunoprecipitation assay protocol was optimized for the anti-I-2 antibody and purified His-tagged I-2, using Protein G Sepharose slurry (Figure 21). The immunoblot analysis indicated that using different elution conditions of the IgG from protein G, by heating the sample (Figure 21a) or by adding an acid solution (Figure 21b), the results are similar. Comparing with the control, corresponding to 100 ng of purified I-2-His, the amount of I-2 immunoprecipitated was also very small. In addition, a non-specific band with 32 kDa corresponding to the protein G was seen in the blot, indicating that Protein G, covalently linked to the beads slurry, detaches from the beads, possible during the boiling and acid elution of the sample. Similar results were obtained using Protein A Sepharose slurry, where a non-specific band with 42 kDa, corresponding to the protein A, was seen in the blot (data not shown).

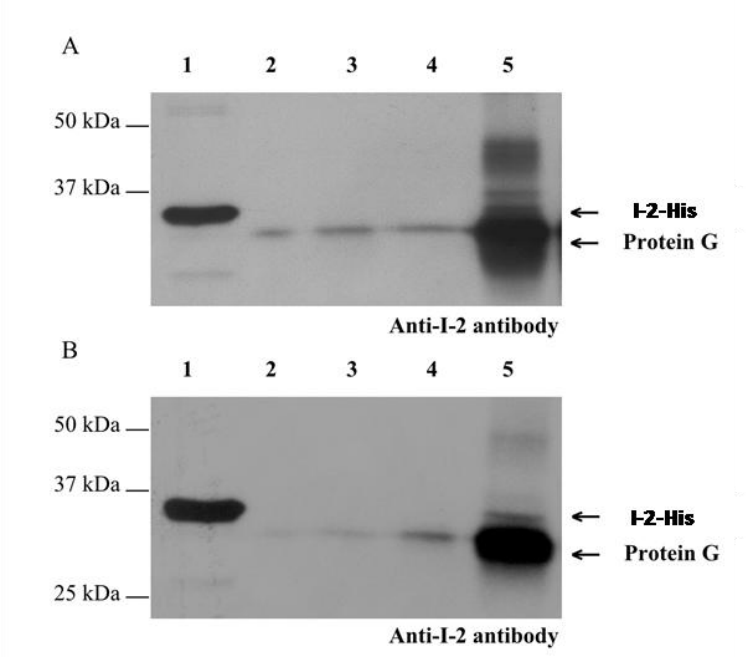


**Figure 21:** Immunoblot analysis of purified I-2-His immunoprecipitated using Protein G Sepharose slurry and anti-I-2 antibody, and immunoblotted with anti-I-2 antibody. Immunoblot comparison of the IgG eluted from protein G by heat at 70 ºC **A**| and by glycin/tris-HCl elution buffer **B**|**.** 1, I-2-His (100 ng); 2-4, washes; 5, I-2-His immunoprecipitated with anti-I-2 antibody.

Because the immunoprecipitation of purified I-2-His was not successful, we tried to apply the immunoprecipitation protocol using Dynabeads® Protein G instead of Protein G Sepharose slurry. The blotting analysis revealed that I-2-His was more successfully immunoprecipitated (Figure 22), despite the loss of I-2 protein during the washing procedure. In the view of these results, the Dynabeads® Protein G procedure will be used for the immunoprecipitation of I-2/I-2L from human sperm samples.

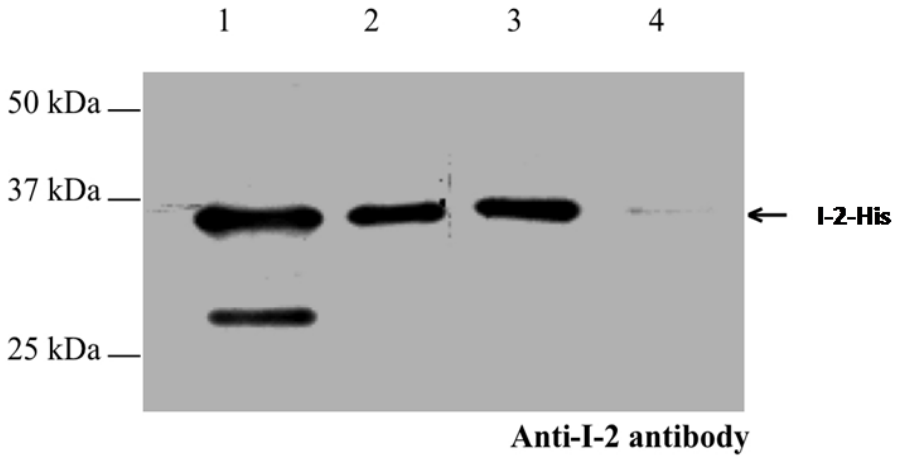


**Figure 22:** Immunoblot analysis of purified I-2-His immunoprecipitated with Dynabeads® Protein G and anti-I-2 antibody, and immunoblotted with anti-I-2 antibody. 1, I-2-His (100 ng)**;** 2, I-2-His immunoprecipitated with anti-I-2 antibody; 3-4, washes.

In order to perceive if it was possible to recover the I-2 and I-2L peptides by mass spectrometry, purified I-2-His (200 ng) and purified I-2L proteins (200 ng), were separated in a 10% SDS-PAGE gel, transferred to a nitrocellulose membrane and revealed with ECL (Figure 23a) or stained with Coomassie blue colloidal (Figure 23b). Then, the band was extracted from the gel for further mass spectrometry analysis. The results indicated that, as expected, purified I-2-His run in the SDS gel with approximately 37 kDa and purified I-2L (previously purified in our laboratory by Ana Vintém) run in the SDS gel with 32 kDa. The amount of I-2 or I-2L proteins for the visualization and in-gel extraction of the bands indicated for further mass spectrometry analysis was 100 ng.

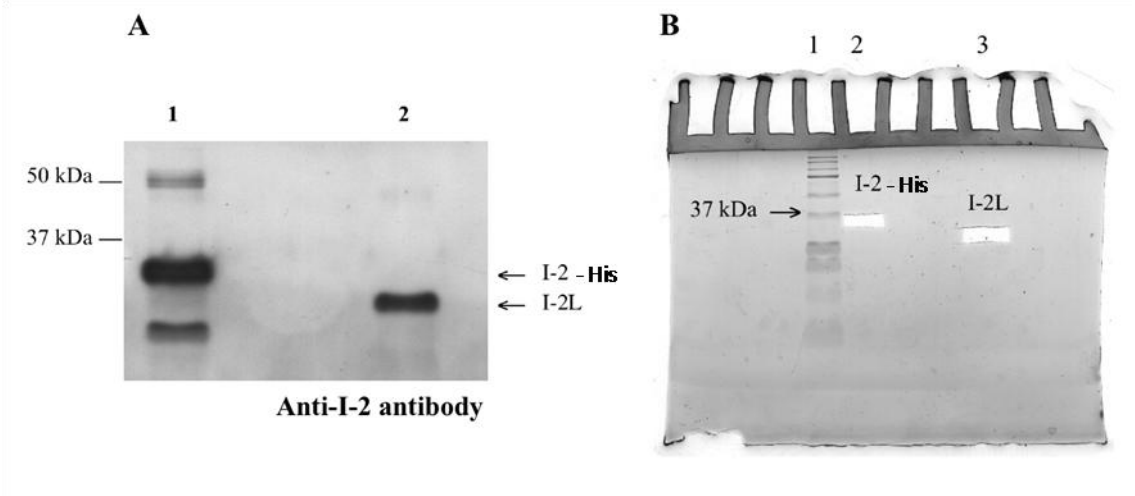


**Figure 23: A** | Immunoblot analysis of purified I-2-His and purified I-2L using anti-I-2 antibody. 1, I-2-His (200 ng); 2, I-2L (200 ng). **B** | Coomassie colloidal blue stained and in-gel extraction of I-2/I-2L band. 1, Precision Plus Protein™ (5 ng); 2, I-2-His (200 ng); 3, I-2L (200 ng).

Taking into account the previous results with purified I-2-His and purified I-2L, sperm cell lysates and immunoprecipitates (IP) were performed using anti-I-2 antibody and these were separated in two different 10% SDS-PAGE gels. One of the gels, loaded with the sperm cell lysates and 40 µl of the IP, was transferred to a nitrocellulose membrane, immunoblotted with anti-I-2 antibody and developed by ECL (Figure 24a). The other gel was loaded with 60 µl of the IP and stained with Coomassie blue colloidal staining solution (Figure 24b). Upon immunoprecipitation with anti-I-2 antibody, a strong band bellow 37 kDa, corresponding to I-2/I-2L protein (32 kDa), was detected by immunoblotting with anti-I-2 antibody (Figure 24a). These results indicated and confirmed that I-2/I-2L is expressed *in vivo* in human sperm, and that can be successfully isolated and purified from the human sperm extract. None I-2/I-2L was detected in the preclearance and washes, indicating that I-2/I-2L present in the sample were immunoprecipitated altogether. These results also demonstrated that I-2/I-2L immunoprecipitated from human sperm extracts run in the SDS gel as a co-migrating species, that are visualized in the immunoblot as a band corresponding to a molecular weight of 32 kDa. All the remaining IP was separated in the Coomassie blue staining gel. However, the band obtained from the staining at 32 kDa, corresponding to I-2/I-2L proteins, was very weak, but still visible, indicating that the amount of protein present may be sufficient for the mass spectrometry analysis (Figure 24b). Additionally, a large band of approximately 50 kDa was also detected in the

immunoprecipitated corresponding to BSA protein used during the immunoprecipitation procedure (Figure 24b).

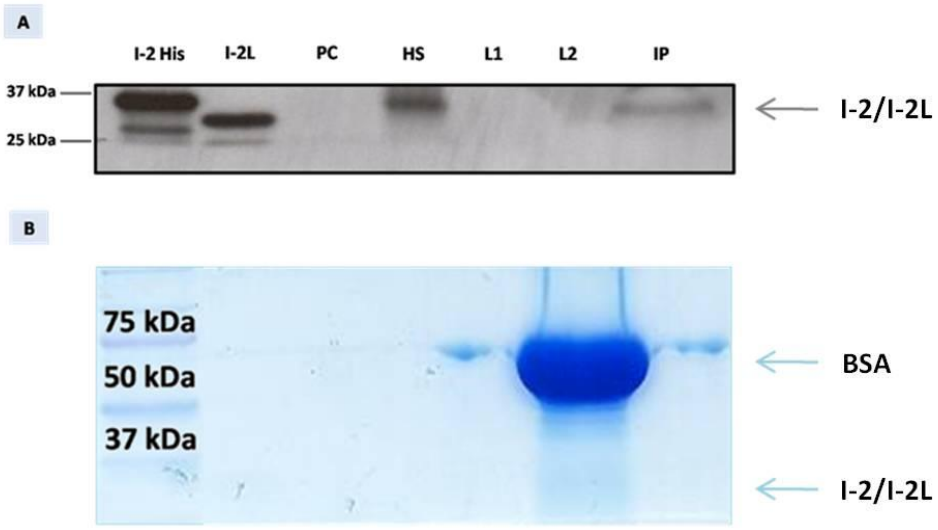


**Figure 24:** Isolation and purification of I-2/I-2L from human sperm extract by immunoprecipitation. **A**|Immunoblot analysis of human sperm extract immunoprecipitated with anti-I-2 antibody and immunoblotted with anti-I-2 antibody. Purified I-2-His (100 ng) and purified I-2L (100 ng) were used as controls. PC, preclearance; HS, human sperm lysate; L1-L2, washes; IP, immunoprecipitated I-2/I-2L with Dynabeads® Protein G. **B**|Coomassie colloidal blue stained 10% SDS gel containing the immunoprecipitated I-2/I-2L (IP) with Dynabeads® Protein G.

### 3.3.4. Discussion

Immunoprecipitation is a reliable technique used to isolate and purify a protein of interest from a sample containing a complex mixture of proteins that works by the formation of antigen-antibody complexes (Sambrook *et al.*, 1989). To address the physiological relevance of PP1γ2-I-2L complex, we attempted to demonstrate *in vivo* that I-2L is expressed in human sperm and that it occurs as a PP1γ2 interacting protein in human sperm. Immunoprecipitations were performed, first with the purified His-tagged I-2 and I-2L proteins, to optimize the immunoprecipitation assay protocol, and then with human sperm extracts using an anti-I-2 antibody followed by immunoblot analysis using anti-I-2 antibody and, in parallel, the analysis and in-gel extraction of the band corresponding to I-2/I-2L stained with Coomassie blue colloidal. The extracted bands were sent for to MS analysis and the peptides obtained from tryptic digestion compared (see section 2.2) in order to validate the amino acid sequence of I-2L obtained from the YTH analysis.

# 4. Discussion and Perspectives

Protein phosphorylation represents one of the most common post-translational modifications in eukaryotes. Protein Serine/Threonine Phosphatase-1 (PP1) catalyzes the majority of eukaryotic protein dephosphorylation reactions in a highly regulated and selective manner. PP1-interacting proteins (PIPs) function as targeting subunits, substrates and/or inhibitors (Bollen *et al.*, 2001; 2010). PIPs form stable complexes with PP1 via degenerate docking motifs, often in the context of structurally disordered interaction domains. PP1 is regulated by more than 100 known PIPs that distinctly and specifically regulate PP1 to enable rapid responses to cellular alterations (Fardilha *et al*., 2010). I-2 belongs to a class of IUPs and has a number of domains that are involved in the interaction of PP1, and interestingly, does not require phosphorylation to inhibit PP1, forming a PP1-I-2 complex that reveals three crucial interaction sites, involving an RVxF-motif, a SILK-sequence and a long α-helix, that covers the active site, preventing PP1 activity. Thus, this binding does not induce conformational changes to PP1, but trigger the release of one or two catalytic metal ions (Bollen *et al.*, 2010; Dancheck *et al*., 2008; Hurley *et al*., 2007).

The importance of PP1-I-2 complex in the regulation of sperm motility has been well documented in the literature (Fardilha *et al*., 2004; Hung and Vijayaraghavan, 2004; Vijayaraghavan *et al.*, 1996; 2000). Sperm cells are terminally differentiated cells that essentially devoid transcriptional and translational activity. Thus, PP1 driven endogenous regulation of protein phosphorylation and sperm motility could represent an important mechanism for the physiological regulation of a cell that encounters dramatically different environments as its journeys through the seminiferous tubules and the female reproductive tract.

In order to find which PP1 partners might be involved in the control of sperm motility, we embarked on a study aimed at defining the testis specific interactomes of PP1γ1 and PP1γ2, the two known alternatively splicing variants of the *PP1γ* gene (Fardilha *et al.*, 2004). To accomplish this aim, exhaustive screens were performed using a human testis cDNA library. Here, we report the discovery of a new PP1 binding protein, termed I-2L, that is 95% identical to I-2 at the amino acid level. I-2L retains the I-2 most important sequences observed for the interaction with PP1 as showed by bioinformatics analysis (Chapter 2), such as the SILK-motif ($^{12}$KGILK$^{16}$), important for the inhibitory capacity of I-2, and the degenerated RVxF-motif ($^{43}$KSQKW$^{47}$) that binds to the hydrophobic groove behind the PP1 catalytic site. Furthermore, I-2L also contains the putative nuclear

localization signal ($^{136}$KKRQFEMKR$^{144}$) indicating that I-2L, can differentially localize to the cytoplasm or nucleus, depending on the phase of the cell cycle (Leach *et al.*, 2002).

The major difference between I-2 and I-2L is the substitution of the main PP1 regulatory residue Thr73 for Pro73 in I-2L sequence. The absence of GSK-3 phosphorylation site at Thr73 in I-2L raises an interesting question: is there an alternative mechanism for the inhibitory control of PP1 holoenzyme by the I-2L that rule out the phosphorylation by GSK-3? Certainly, several studies demonstrated that PP1γ2 and GSK-3 activities are two- and six- fold higher, respectively, in immature caput compared to motile epididymal sperm. This raises another question: is the inhibition by I-2L more effective in the epididymal cauda that could explain the unidirectional acquisition of sperm motility along the epididymal tract? Indeed, variation in only nine amino-acids (5%) introduces differences in the signal transduction regulation of these almost identical proteins. This could confer completely different functions to the PP1c-I-2 and PP1c-I-2L complexes, specifically in what concerns to sperm motility (Figure 9). Considering the above data, it seems reasonable to hypothesize a possible role for I-2L functions in sperm. Being associated with PP1γ2 in sperm tail, it might be involved in the control of sperm motility. Our theoretical model (Figure 25) indicates that, along the epididymis, I-2 concentration decreases and I-2L increases, leading to a reduction in PP1 activity from the caput to the caudal portion of the epididymis. This would be an extremely good explanation to the unidirectional acquisition of sperm motility.

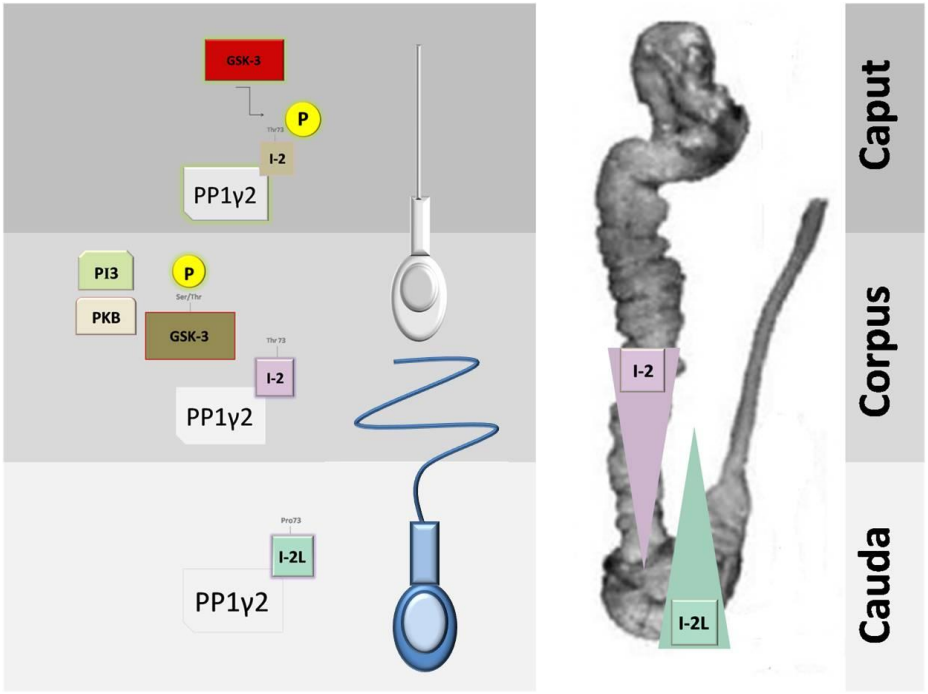


**Figure 25:** Model of a putative regulation mechanism of the PP1c-I-2L complex and sperm motility. I-2L expression increases along the epididymis, and by contrary, I-2 expression decreases. This could lead to the formation of a PP1c-I-2L constitutive inactive complex in caudal motile sperm that could not be reactivated by phosphorylation of Thr73 residue by GSK-3 kinase, once it is absent in I-2L.

The presence of I-2/I-2L in human sperm was confirmed by immunoblot and immunocytochemistry analysis, using a specific anti-I-2 antibody which recognizes both proteins. Our results demonstrated that I-2/I-2L is highly expressed in human sperm together with PP1γ2. Additionally, the results indicated that I-2/I-2L co-localize endogenously with the PP1γ2 isoform in the principal-piece and middle-piece of spermatozoa flagellum, consistent with the role of PP1-(I-2/I-2L) in the sperm motility.

Our results also demonstrated that I-2/I-2L co-localizes with PP1γ2 in the postacrosomal and equatorial segment of the spermatozoa head indicated that I-2L might be present in cytoplasm being essential for the acrosome reaction. The presence of a putative PKC phosphorylation site indicates that I-2L may be an intermediate between calcium signaling and PP1γ2 regulation of sperm acrosome reaction (Figure 26).

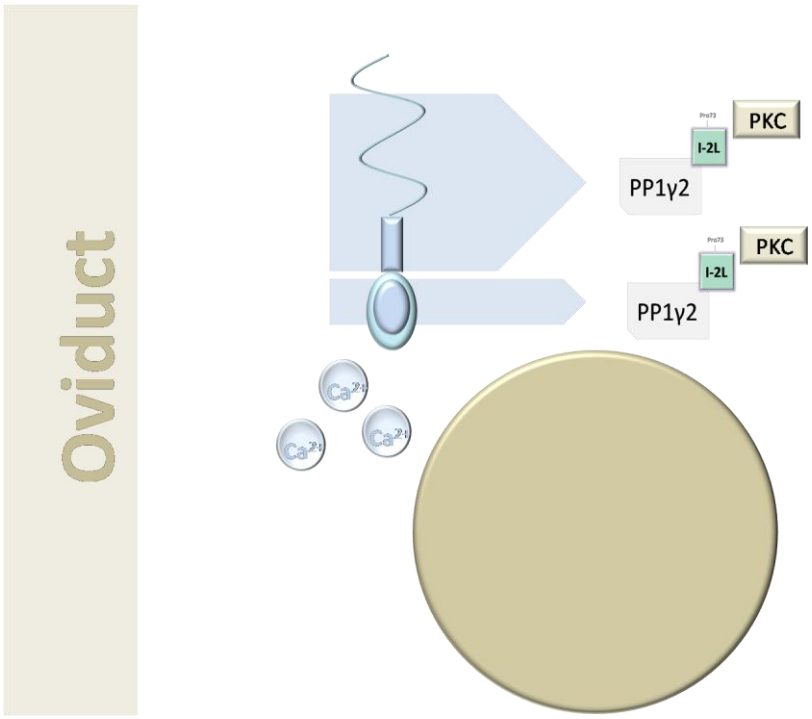


**Figure 26:** Schematic representation of the co-localization of I-2L with PP1γ2 in the postacrosomal and equatorial segment of the spermatozoa head. The presence of I-2L in the cytoplasm of the postacrosomal and equatorial segment may be essential for the spermatozoa acrosome reaction. The phosphorylation of I-2L by PKC may activate the PP1γ2 that may act in the opening of the calcium channels in the plasmatic membrane, promoting the release of calcium to the cytosol.

Sperm undergo acrosome reaction when they bind to the egg´s zona pellucida, enabling the sperm to penetrate the egg. Prior to this binding, the spermatozoa undergo in the female reproductive tract a series of biochemical transformations, involving the elevation of cytosolic calcium and a signal transduction cascade that culminate in the activation of cAMP/PKA and PKC that leads to the sperm acrosome reaction. PKA and IP3 activate the calcium channels in the outer acrosome membrane, resulting in membrane fusion and acrosome reaction. PKC opens the calcium channel in the plasma membrane increasing the concentration of cytosolic calcium that promotes the fusion between the plasma membrane and the outer acrosome membrane (Breitbart, 2002; Turner, 2003). Through bioinformatics analysis we concluded that I-2//I-2L have three putative phosphorylation sites for PKC at the Ser7, Ser41 and Ser44 residues, indicating that I-2L may be involved in the acrosome reaction, as suggested by our immunocytochemical

results. Our hypothesis is that the phosphorylation of I-2L by PKC may activate the PP1γ2 that may regulate the opening of the calcium channels in the plasmatic membrane, promoting the release of calcium to the cytosol (Figure 26).

We proposed that I-2L is an expressed gene producing a functional protein that interacts with the testis- and sperm- specific PP1γ2 isoform, since it was identified from a human testis cDNA library using PP1γ isoforms as baits. However, the similarities between I-2 and I-2L in terms of nucleotides and amino acids are enormous, which makes it difficult to distinguish them. Our immunoblot and immunocytochemistry results did not allow us to reach any conclusions regarding the expression of I-2L protein alone. Therefore, with the proposal of confirming that I-2L is expressed and is a PP1γ2-interacting protein in human sperm, and also to addressing the physiological relevance of PP1γ2-I-2L *in vivo*, we immunoprecipitated I-2/I-2L from human sperm to further analyze the peptide *fingerprint* by mass spectrometry (MS). Through bioinformatics analysis, we concluded that the digestion with trypsin originates different patterns of cleavage in the amino acid I-2 and I-2L sequences, allowing the distinction between I-2 and I-2L as two different proteins expressed by two paralogue genes. Interestingly, the identification of I-2L by mass spectrometry opens new perspectives for the study of the physiological role of the PP1γ2-I-2L complex in the acquisition of sperm motility, where protein phosphorylation may constitute a pivotal regulatory mechanism. It will be interesting to evaluate the occurrence of I-2L in caput and caudal sperm assessing the formation of PP1γ2-I-2L constitutive inactive complex in caudal motile sperm (Figure 25).

Another relevant way to access the relevance of I-2 and I-2L would be to attempt the *in vivo* overexpression of I-2 and I-2L mice with *PGK2* promotor that is directed in a strictly tissue-manner in meiotic spermatocytes and postmeioic spermatides during spermatogenesis in eutherian mammals (Zhang *et al.*, 1999). Indeed, I-2 or I-2L would be expressed only in testis and consequences of their expression would be evaluated on spermatogenesis and spermiogenesis. Thus, the hypothesis of the relationship between I-2L and the inactivation of PP1γ2 activity in caudal sperm seems worthwhile exploring in the future.

# 5. References

**Agarwal-Mawal**, A., Paudel, H. K. 2001. Neuronal cdc2-like protein kinase (cdk5/p25) is associated with protein phosphatase 1 and phosphorylates inhibitor-2. *The Journal of Biological Chemistry*, 276 (26): 23712-23718.

**Ahmad**, Z., Lee, F-T., DePaoli-Roach, A., Roach, P. J. 1984. Phosphorylation of glycogen synthase by $Ca^{2+}$-and phospholipid-activated protein kinase (Protein kinase C). *The Journal of Biological Chemistry*, 259 (14): 8743-8747.

**Balakirev**, E. S., Ayala, F. J. 2003. Pseudogenes: are they "junk" or functional DNA? *Annual Review of Genetics*, 37: 123-51.

**Balakirev**, E. S., Ayala, F. J. 2004. Pseudogenes: structure conservation, expression, and functions. *Zhurnal Obshchei Biologii*, 65 (4): 306-21.

**Berggard**, T., Linse, S., James, P. 2007. Methods for the detection and analysis of protein-protein interactions. *Proteomics*, 7: 2833-42.

**Bollen**, M. 2001. Combinatorial control of protein phosphates-1. *Trends in Biochemical Sciences*, 26: 426-31.

**Bollen**, M., Peti, W., Ragusa, M. J., Beullens, M. 2010. The extended PP1 toolkit: designed to create specificity. *Trends in Biochemical Sciences*, doi: 10.1016/j.tibs.2010.03.02.

**Breitbart**, H. 2002. Intracellular calcium regulation in sperm capacitation and acrosomal reaction. *Molecular and Cellular Endocrinology*, 187: 139-144.

**Ceulemans**, H., Stalmans, W., Bollen, M. 2002. Regulatory-driven functional diversification of protein phosphatase-1 in eukaryotic evolution. *Bioessays*, 24: 371-81.

**Ceulemans**, H., Bollen, M. 2004. Functional diversity of protein phosphatase-1, a cellular economizer and reset button. *Physiological Reviews*, 84: 1-39.

**Chrakrabarti**, R., Kline, D., Lu, J., Orth, J., Pilder, S., Vijayaraghavan, S. 2007. Analysis of *Ppp1cc*-null mice suggests a role for PP1gamma2 in sperm morphogenesis. *Biology of Reproduction*, 76: 992-1001.

**da Cruz e Silva**, E. F., Fox, C. A., Quimet, C. C., Gustafson, E., Watson, S. J., Greengard, P. 1995. Differential expression of protein phosphatase 1 isoforms in mammalian brain. *The Journal of Neuroscience*, 15 (5): 3375-3389.

**Dancheck**, B., Nairn, A. C., Peti, W. 2008. Detailed structural characterization of unbound protein phosphatase 1 inhibitors. *Biochemistry*, 47 (47): 12346-12356.

**De Jonge**, C., Barrat, C. 2006. The sperm cell: production, maturation, fertilization, regeneration. 1st ed. Cambridge University Press. UK. pp 1-169.

**Dravland,** J. E., Mortimer, D. 1985. A simple discontinuous, percoll gradients procedure for washing human spermatozoa. *IRCS Medical Science*, 13:16.

**Eto**, M., Elliott, E., Prichett, T. D., Brautigan, D. L. 2002. Inhibitor-2 regulates protein phosphatase-1 complexed with NimA-related kinase to induce centrosome separation. *The Journal of Biological Chemistry*, 277 (46): 44013-44020.

**Fardilha**, M., Wu, W., Sá, R., Fidalgo, S., Sousa, C., Mota, C., da Cruz e Silva, O., da Cruz e Silva, E. F. 2004. Alternative spliced protein variants as potential therapeutic targets for male infertility and contraception. *Annals of the New York Academy of Sciences*, 1030: 468-478.

**Fardilha**, M., Esteves, S. L. C., Korrodi, L. M. G, da Cruz e Silva, O. A. B., da Cruz e Silva, E. F. 2010. The physiological relevance of protein phosphatase 1 and the interacting proteins to health and disease. *Current Medicinal Chemistry* (in press).

**Gupta**, R. C., Mishra, S., Yang, K-P-. Sabbah, H. N. 2005. Reduced inhibitor 1 and 2 activity is associated with increased protein phosphatase type 1 activity in left ventricular myocardium of one-kidney, one-clip hypertensive rats. *Molecular and Cellular Biochemistry*, 269: 49-57.

**Helpes**, N. R., Cohen, P. T. W. 1999. *Drosophila melanogaster* protein phosphatase inhibitor-2: identification of the site important for PP1 inhibition. *FEBS Letters*, 463: 72-76.

**Hendrickx**, A., Beullens, M., Ceulemans, H., Abt, T. D., Eynde, A. V., Nicolaescu, E., Lesage, B., Bollen, M. 2009. Docking motif-guided mapping of the interactome of protein phosphatase-1. *Chemistry & Biology*, 16: 365-371.

**Hirotsune**, S., Yoshida, N., Chen, A., Garrett, L., Sugiyama, F., Takahashi, S., Yagami, K-I., Boris-Wynshaw, A., Yoshiki, A. 2003. An expressed pseudogene regulates the messenger-RNA stability of its homologous coding gene. *Nature*, 423: 91-100.

**Holmes**, C. F. B., Kuret, J., Chisholm, A. A., Cohen, P. 1986. Identification of the sites on rabbit skeletal muscle protein phosphatase inhibitor-2 phosphorylated by casein kinase-II. *Biochimica et Biophysica Acta*, 870: 408-416.

**Honkanen**, R. E., Golden, T. 2002. Regulators of serine/threonine protein phosphatases at the dawn of a clinical era? *Current Medical Chemistry*, 9: 2055-75.

**Huang**, F. L. and Glinsmann, W. H. 1976. Separation and characterization of two phosphorylase phosphatase inhibitors from rabbit skeletal muscle. *European Journal of Biochemistry*, 70: 419-426.

**Huang**, Z., Khatra, B., Bollen, M., Carr, D. W., Vijayaraghavan, S. 2002. Sperm PP1γ2 is regulated by a homologue of the yeast protein phosphatase binding protein sds22. *Biology of Reproduction*, 67: 1936-1942.

**Huang**, Z., Vijayaraghavan, S. 2004. Increased phosphorylation of a distinct subcellular pool of protein phosphatase, PP1γ2, during epididymal sperm maturation. *Biology of Reproduction*, 70: 439-447.

**Hurley**, T. D., Yang, J., Zhang, L., Goodwin, K. D., Zou, Q., Cortese, M., Dunker, A. K., DePaoli-Roach, A. A. 2007. Structural basis for regulation of protein phosphatase 1 by inhibitor-2. *The Journal of Biological Chemistry*, 282 (39): 28874-28883.

**Ingebritsen**, T. S., Cohen, P. 1983. Protein phosphatases: properties and roles in cellular regulation. *Science*, 221: 331-338.

**King**, T. D., Gandy, J. C., Bijur, G. N. 2006. The protein phosphatase-1/inhibitor-2 complex differentially regulates GSK3 dephosphorylation and increases sarcoplasmic/endoplasmic reticulum calcium ATPase2 levels. *Experimental Cell Research*, 312: 3693-3700.

**Kirchhefer**, U., Baba, A. H., Boknik, P., Breeden, K. M., Mavilla, N., Brüchen, N., Justus, I., Matus, M., Schmitz, W., DePaoli-Roach, A. A., Neumann, J. 2005. Enhanced cardiac function in mice overexpressing protein phosphatase inhibitor-2. *Cardiovascular Research*, 68: 98-108.

**Koegl**, M., Uetz, P. 2008. Improving yeast two-hybrid screening systems. *Briefings in Functional Genomics and Proteomics*, 6 (4): 302-312.

**Küpker**, W., Diedrich, K., Edwards, R. G. 1998. Principles of mammalian fertilization. *European Society for Human Reproduction & Embryology*, 13: 20-32.

**Lalonde**, S., Ehrhardt, D. W., Loqué, D., Chen, J., Rhee, S. Y., Frommer, W. B. 2008. Molecular and cellular approaches for the detection of protein-protein interactions: latest techniques and current limitations. *The Plant Journal*, 53: 610-635.

**Leach**, C., Eto, M., Brautigan, D. L. 2002. Domains of type 1 protein phosphatase inhibitor-2 required for nuclear and cytoplasmic localization in response to cell-cell contact. *Journal of Cell Science*, 115: 3739-3742.

**Leach**, C., Shenolikar, S., Brautigan, D. L. 2003. Phosphorylation of phosphatase inhibitor-2 at centrosomes during mitoses. *The Journal of Biological Chemistry*, 278 (28): 26015-26020.

**Li**, M., Satinover, D. L., Brautigan, D. L. 2007. Phosphorylation and function of inhibitor-2 family of proteins. *Biochemistry*, 46: 2380-2389.

**Lishko**, P. V., Botchkina, I. L., Fedorenko, A., Kirichok, Y. 2009. Acid extrusion from human spermatozoa is mediated by flagellar voltage-gated proton channel. *Cell*, 140: 327-337.

**Lodge**, J., Lund, P., Minchin, S. 2007. Gene cloning: principles and application. 1st ed. Taylor & Francis Group. UK. pp 224-359.

**Morfini**, G., Szebeny, G., Brown, H., Pant, H. C., Pigino, G. DeBoer, S., Beffert, U., Brady, S. T. 2004. A novel CDK5-dependent pathway for regulating GSK-3 activity and kinesin-driven motility in neurons. *The EMBO Journal*, 23: 2235-2245.

**Mortimer**, D. 2000. Sperm preparation methods. *Journal of Andrology*, 21 (3): 357-365.

**Osawa**, Y., Nakagama, H., Shima, H., Sugimura, T., Nagao, M. 1996. Identification and characterization of three isotypes of protein phosphatase inhibitor-2 and their expression profiles during testis maturation in rats. *FEBS*, 242: 793-798.

**Parrish**, J. R., Gulyas, K. D., Finley, R. L. 2006. Yeast two-hybrid contributions to interactome mapping. *Current Opinion in Biotechnology*, 17: 387-393.

**Park**, I-K., Roach, P., Bondor, J., Fox, S. P., DePaoli-Roach, A. A. 1994. Molecular mechanism of the synergistic phosphorylation of phosphatase inhibitor-2. *The Journal of Biological Chemistry*, 269 (2): 944-954.

**Puntervoll**, P., Linding, R., Gemünd, C., Chabanis-Davidson, S., Mattingsdal, M., Cameron, S., Martin, D. M. A., Ausiello, G., Brannetti, B., Constantine, A., Ferrè, F., Maselli, V., Via, A., Cesareni, G., Diella, F., Superti-Furga, G., Wyrwicz, L., Ramu, C., McGuigan, C., Gudavalli, R., Letunic, I., Bork, P., Rychlewski, L., Küster, B., Helmer-Citterich, M., Hunter, W. N., Aaland, R., Gibson, T. J. 2003. EML server: a new resource for investigation short functional sites in modular eukaryotic proteins. *Nucleic Acids Research*, 31 (13): 3625-3630.

**Roach**, P., Roach, P. J., DePaoli-Roach, A. A. 1985. Phosphoprotein phosphatase inhibitor-2. *The Journal of Biological Chemistry*, 260 (10): 6314-6317.

**Sakashita**, G., Shima, H., Komatsu, M., Urano, T., Kikuchi, A., Kikuchi, K. 2003. Regulation of type 1 protein phosphatase/inhibitor-2 complex by glycogen synthase kinase-3β in intact cells. *Journal of Biochemistry*, 133: 165-171.

**Sambrook**, J., Fritsch, E. F., Maniatis, T. 1989. Molecular cloning: a laboratory manual. 2nd ed. Cold Spring Harbor Laboratory Press. USA. pp 1847-1870.

**Satinover**, D., Leach, C. A., Stukenberg, P. T., Brautigan, D. L. 2004. Activation of Aurora-A kinase by protein phosphatase inhibitor-2, a bifunctional signaling protein. *PNAS*, 101 (23): 8625-8630.

**Si**, Y., Okuno, M. 1999. Role of tyrosine phosphorylation of the flagelar proteins in hamster sperm hyperactivation. *Biology of Reproduction*, 62: 240-246.

**Smith**, G. D., Wolf, D. P., Trautman, K. C., da Cruz e Silva, E. F., Greengard, P., Vijayaraghavan, S., 1996. Primate sperm contain phosphatase 1, a biochemical mediator of motility. *Biology of Reproduction*, 54: 719-727.

**Smith,** G. D., Wolf, D. P., Trautman, K. C., Vijayaraghavan, S. 1999. Motility potential of macaque epididymal sperm: The role of protein phosphatase and glycogen synthase kinase-3 activities. *Journal of Andrology*, 20 (1): 47-53.

**Sun**, C., Orozco, O., Choi, E., Garben, E., Tizard, R., Szack, S., Sanicola, M., Carulli, J. P. 2008. CRIPTO3, a presumed pseudogene, is expressed in cancer. *Biochemical and Biophysical Research Communications*, 377 (1): 215-220.

**Terry-Lorenzo**, R. T., Elliot, E., Weiser, D. C., Prickett, T. D., Brautigan, D. L., Shenolikar, S. 2002. Neurabins recruit protein phosphatase-1 and inhibitor-2 to the actin cytoskeleton. *The Journal of Biological Chemistry*, 277 (48): 46535-46543.

**Turner**, R. M. 2003. Tales from the tail: What do we really know about sperm motility? *Journal of Andrology*, 24 (6): 790-803.

**Vijayaraghavan**, S., Sephens, D. T., Trautman, K., Smith, G. D., Khatra, B., da Cruz e Silva, E. F., Greengard, P. 1996. Sperm motility development in the epididymis is associated with decreased glycogen synthase kinase-3 and protein phosphatase 1 activity. *Biology of Reproduction*, 54: 709-718.

**Vijayaraghavan**, S., Mohan, J., Gray, H., Khatra, B., Carr, D. W. 2000. A role for phosphorylation of glycogen synthase kinase-3α in bovine sperm motility regulation. *Biology of Reproduction*, 62: 1647-1654.

**Virshup**, D. M., Shenolikar, S. 2009. From promiscuity to precision: Protein phosphatases get a makeover. *Molecular Cell*, 33: 537-545.

**Wang**, Q. M., Park, I-K., Fiol, C. J., Roach, P. J., DePaoli-Roach, A. A. 1994. Isoform differences in substrate recognition by glycogen synthase kinase 3α and 3β in the phosphorylation of phosphatase inhibitor 2. *Biochemistry*, 33: 143-147.

**Wakula**, P., Beullens, M., Ceulemans, H., Stalmans, W., Bollen, M. 2003. Degeneracy and function of the ubiquitous RVxF motif that mediates binding to protein phosphatse-1. *The Journal of Biological Chemistry,* 278 (21): 18817-18823.

**Wang**, Q. M., Guan, K-L., Roach, P. J., DePaoli-Roach, A. A. 1995. Phosphorylation and activation of the ATP-Mg-dependent protein phosphatase by the mitogen-activated protein kinase. *The Journal of biological chemistry*, 270 (31): 18352-18358.

**Wang**, W., Brautigan, D. L. 2008. Phosphatase inhibitor 2 promotes acetylation of tubulin in the primary cilium of human retinal epithelial cells. *BML Cell Biology*, 9: 62.

**Wu**, W., Baxter, J. E., Wattam, S. M., Hayward, D. G., Fardilha, M., Knebel, A., Ford, E. M., da Cruz e Silva, E. F., Fry, A. M. 2007. Alternative splicing controls nuclear translocation of the cell cycle-regulated Nek2 kinase. *The Journal of Biological Chemistry*, 282(36): 26431-2644.

**Yamada**, M., Ikena, Y., Yano, M., Yoshimuro, K., Nishino, S., Aoyama, H., Wang, L., Aoki, H., Matsuzaki, M. 2006. Inhibition of protein phosphatase 1 by inhibitor-2 gene delivery ameliorates heart failure progression in genetic cardiomyopathy. *FASEB Journal*, 20: 1197-1200.

**Yang**, P., Fox, L., Colbran, R. J., Sale, W. S. 2000. Protein phosphatases PP1 and PP2A are located in distinct positions in the *Chlamydomonas* flagellar axoneme. *Journal of Cell Science*, 113: 91-102.

**Zhang**, Z., Bai, G., Zhao, S., Nagao, M., Lee, E. Y. 1993. Expression and characterization of rat protein phosphatases-1 alpha, -1 gamma 1, -1 gamma 2, and -1 delta. *Archives of Biochemistry and Biophysics*, 303(2): 402-6.

**Zhang**, L. P., Stroud, J., Eddy, C. A., Walter, C. A., McCarrey, J. R. 1999. Multiple elements influence transcriptional regulation from the human testis-specific *PGK2* promoter in transgenic mice. *Biology of Reproduction*, 60: 1329-1337.

# Appendix

**SDS-PAGE and Immunoblotting Solutions**

LGB (Lower Gel Buffer)

To 900 ml of deionized $H_2O$ add:
Tris 181.65 g
SDS 4 g
Mix until the solutes have dissolved. Adjust the pH to 8.9 and adjust the volume to 1L with deionized $H_2O$.

UGB (Upper Gel Buffer)

To 900 ml of deionized $H_2O$ add:
Tris 75.69 g
Mix until the solute has dissolved. Adjust the pH to 6.8 and adjust the volume to 1L with deionized $H_2O$.

30% Acrylamide/0.8% Bisacrylamide

To 70 ml of deionized $H_2O$ add:
Acrylamide 29.2 g
Bisacrylamide 0.8 g
Mix until the solutes have dissolved. Adjust the volume to 100 mL with deionized $H_2O$. Filter through a 0.2 μm filter and store at 4 °C.

10% APS (ammonium persulfate)

In 10 ml of deionized $H_2O$ dissolve 1 g of APS.

10% SDS (sodium dodecilsulfate)

In 10 ml of deionized $H_2O$ dissolve 1 g of SDS.

(4x) Loading Gel Buffer

| | |
|---|---|
| 1 M Tris solution (pH 6.8) | 2.5 ml (250 mM) |
| SDS | 0.8 g (0.8%) |
| Glycerol | 4 ml (40%) |
| β-Mercaptoethanol | 2 ml (2%) |
| Bromophenol blue | 1 mg (0.01 %) |

Adjust the volume to 10 ml with deionized $H_2O$. Store in darkness at RT.

1 M Tris (pH 6.8) solution

To 150 ml of deionized $H_2O$ add:

Tris base 30.3 g

Adjust the pH to 6.8 and adjust the final volume to 250 ml.

10x Running Buffer

| | |
|---|---|
| Tris | 30.3 g (250 mM) |
| Glycine | 144.2 g (2.5 M) |
| SDS | 10 g (1%) |

Dissolve in deionized $H_2O$, adjust the pH to 8.3 and adjust the volume to 1 L.

10x Transfer buffer

| | |
|---|---|
| Tris | 3.03 g (25 mM) |
| Glycine | 14.41 g (192 mM) |

Mix until solutes dissolution. Adjust the pH to 8.3 with HCl and adjust the volume to 800 ml with deionized $H_2O$. Just prior to use add 200 ml of methanol (20%).

10x TBS (Tris buffered saline)

Tris 12.11 g (10 mM)

NaCl 87.66 g (150 mM)

Adjust the pH to 8.0 with HCl and adjust the volume to 1 L with deionized $H_2O$.

10x TBST (TBS + Tween)

Tris 12.11 g (10 mM)

NaCl 87.66 g (150 mM)

Tween 20 5 ml (0.05%)

Adjust the pH to 8.0 with HCl and adjust the volume to 1 L with deionized $H_2O$.

**Coomassie blue staining solutions**

Fixation solution

Methanol 400 ml

Acetic acid 100 ml

Adjust the volume to 1 L with deionized $H_2O$.

Staining solution

Coomassie Blue G250 1.2 g

Methanol 200 ml

Adjust the volume to 1 L with deionized $H_2O$.

Distaining solution

Methanol 250 ml

Adjust the volume to 1 L with deionized $H_2O$.

**Immunocytochemistry solutions**

1x PBS

For a final volume of 500 ml, dissolve one pack of BupH Modified Dulbecco´s Phosphate Buffered Saline Pack (Pearce) in deionized $H_2O$. Final composition,

8 mM Sodium Phosphate
2 mM Potassium Phosphate
40 mM NaCl
10 mM KCl
Sterilize by filtering through a 0.2 µm filter and store at 4 ºC.

10x 1 mg/ml Poly-L-ornithine solution

To a final volume of 100 ml, dissolved in ionised $H_2O$ 100 mg of poly-L-ornithine.

4% Paraformaldehyde

For a final volume of 100 ml, add 4 g of paraformaldehyde to 25 ml of deionized $H_2O$. Dissolve by heating the mixture at 58 ºC while stirring. Add 1-2 drops of 1 M NaOH to clarify the solution and filter (0.2 µm filter). Add 50 ml of 2x PBS and adjust the volume to 100 ml with deionized $H_2O$.

**Immunoprecipitation solutions**

1x PBS 3% BSA Buffer

For a final volume of 10 ml, add 0.3 g of BSA to 10 ml of 1x PBS and dissolve.

1x PBS 3% BSA Buffer + Protease inhibitors

Add to 4 ml of 1x PBS 3% BSA buffer the following quantities for a final volume of 5 ml:

| | |
|---|---|
| Pepstatin A (1 mg/ml stock solution in DMSO) | 23.8 µl |
| Leupeptin (5 mg/ml stock solution) | 0.72 µl |
| Benzamidine (200 mM stock solution) | 180 µl |
| Aprotinin (2.1 mg/ml stock solution) | 43.2 µl |
| PMSF (10 mM stock solution) | 176 µl |

**Spermatozoa purification solution**

**NCB stock solutions**

10x $CaCl_2$

For a final volume of 10 ml, add 0.027 g of $CaCl_2$ to deionized $H_2O$. Dissolve and filter (0.2 µm filter) the solution.

10x KCl

For a final volume of 10 ml, add 0.04 g of KCl to deionized $H_2O$.

10x $MgSO_4.7H_2O$

For a final volume of 10 ml, add 0.02 g of $MgSO_4.7H_2O$ to deionized $H_2O$.

10x NaCl

For a final volume of 10 ml, add 0.680 g of NaCl to deionized $H_2O$.

10x $NaHPO_4$

For a final volume of 10 ml, add 0.016 g of $NaHPO_4$ to deionized $H_2O$.

10x D(+)-Glucose

For a final volume of 10 ml, add 0.1 g of D(+) glucose to deionized $H_2O$

10x Na piruvate

For a final volume of 10 ml, add 0.03 g of Na piruvate to deionized $H_2O$.

10x Na lactate

For a final volume of 10 ml, add 0.468 g of Na lactate to deionized $H_2O$.

10x Hepes

For a final volume of 10 ml, add 0.0595 g of Hepes to deionized $H_2O$.